DE), polytetrafluoroethylene, or pericardium might offer significant advantages.

Biomaterial Implantation

The two main purposes of implanting biomaterials are to enhance angiogenesis and to create cardiac tissue in situ by inducing stem cell migration to the scaffold. Supporting this strategy, several reports have shown that resident cells recruited to the injured heart can create new muscle and vascular tissue [75–77].

Gaballa and colleagues [78] reported that implanting collagen type I into a rat myocardial infarction model induced neoangiogenesis and reduced LV remodeling. Biodegradable polyester urethane urea implantation into a rat infarction model improved systolic function and the thickness of the LV wall, and smooth muscle cells with a histologically contractile phenotype were found in the implanted site [79]. The implantation of a porous collagen scaffold enhanced the recruitment of neural crest cells to the implanted patches, even though the frequency of cardiogenic stem cells in the cryoinjured heart is rare compared with the intact heart. Moreover, Western blot analysis showed the expression of smooth muscle and endothelial cell markers but not of cardiomyocytes [80].

Ota and colleagues [81] implanted an ECM patch made from porcine urinary bladder into the porcine right ventricle (RV) wall and detected factor VIII-positive and α-smooth muscle actin-positive cells. An ECM patch derived from porcine urinary bladder was also implanted into the RV free wall in dogs, and the remodeled tissue contained approximately 30% cardiomyocytes [82], but it is not known whether they represented the recruitment of residual stem cells or of stem cells derived from bone marrow.

Interestingly, Robinson and colleagues [83] implanted an ECM patch derived from urinary bladder into a porcine infarction model and detected α-smooth muscle actin-positive cells 1 month after implantation, but at 3 months, the cells derived from the ECM patch were similar to those of normal myocardium by flow cytometry analysis. The mechanism, improvement in cardiac function, and long-term results were not reported. An ECM-derived myocardial patch was implanted into a canine RV with a defect extending the full thickness of the RV wall, which led to improvements in regional systolic and diastolic function, compared with a Dacron patch, and to the presence of cardiomyocytes [84].

Acellular bovine pericardium with a porous structure affixed to genipin was implanted into the RV of a rat model, and histologic examination revealed smooth muscle cells, neomuscle fibers, neoglycosaminoglycans, and neocapillaries in the implanted tissue, but myocytes were not seen [85]. This strategy may interest researchers in the mechanisms of stem cell migration and differentiation.

In this review, we surveyed many exciting topics in myocardial generation therapy in which cardiac surgeons are currently interested. Remarkable progress has been made in cell-based treatments, including cellular cardiomyoplasty and tissue cardiomyoplasty, in a very short period of time. Many researchers and clinicians are enthusiastic about developing new technologies to treat currently intractable heart disease and examining the mechanisms of these techniques from the physiologic, cellular, histologic, and functional points of view. Owing to such studies, some techniques have already been applied clinically, but much remains to be learned, particularly because the technology is still rudimentary at the basic research and clinical levels. The field of clinical myocardial regenerative therapy is just emerging, however, and now is the time for cardiac surgeons to examine ways to promote the assimilation of basic achievements into routine clinical therapy.

This study was supported by the Banyu Fellowship Program sponsored by Banyu Life Science Foundation International.

References

1. Akutsu T, Dreyer B, Kolff WJ. Polyurethane artificial heart valves in animals. J Appl Physiol 1959;14:1045–8.
2. Barnard CN. The operation. A human cardiac transplant: an interim report of a successful operation performed at Groote Schuur Hospital, Cape Town. S Afr Med J 1967;41:1271–4.
3. El-Banayosy A, Korfer R, Arusoglu L, et al. Device and patient management in a bridge-to-transplant setting. Ann Thorac Surg 2001;71:S98–102; discussion S114–5.
4. Piccione W Jr. Bridge to transplant with the HeartMate device. J Card Surg 2001;16:272–9.
5. Birks EJ, Tansley PD, Hardy J, et al. Left ventricular assist device and drug therapy for the reversal of heart failure. N Engl J Med 2006;355:1873–84.
6. Rose EA, Gelijns AC, Moskowitz AJ, et al. Long-term mechanical left ventricular assistance for end-stage heart failure. N Engl J Med 2001;345:1435–43.
7. Mancini DM, Beniaminovitz A, Levin H, et al. Low incidence of myocardial recovery after left ventricular assist device implantation in patients with chronic heart failure. Circulation 1998;98:2383–9.
8. Menasche P, Alfieri O, Janssens S, et al. The Myoblast Autologous Grafting in Ischemic Cardiomyopathy (MAGIC) trial: first randomized placebo-controlled study of myoblast transplantation. Circulation 2008;117:1189–200.
9. Strauer BE, Brehm M, Zeus T, et al. Repair of infarcted myocardium by autologous intracoronary mononuclear bone marrow cell transplantation in humans. Circulation 2002;106:1913–8.
10. Haverich A. Tissue engineering. Eur J Cardiothorac Surg 2004;26(suppl 1):S59–60; discussion S60–1.
11. Iwai S, Sawa Y, Ichikawa H, et al. Biodegradable polymer with collagen microsponge serves as a new bioengineered cardiovascular prosthesis. J Thorac Cardiovasc Surg 2004; 128:472–9.
12. Ozawa T, Mickle DA, Weisel RD, et al. Histologic changes of nonbiodegradable and biodegradable biomaterials used to repair right ventricular heart defects in rats. J Thorac Cardiovasc Surg 2002;124:1157–64.
13. Akins RE, Boyce RA, Madonna ML, et al. Cardiac organogenesis in vitro: reestablishment of three-dimensional tissue architecture by dissociated neonatal rat ventricular cells. Tissue Eng 1999;5:103–18.
14. Kelm JM, Ehler E, Nielsen LK, et al. Design of artificial myocardial microtissues. Tissue Eng 2004;10:201–14.

15. Baar K, Birla R, Boluyt MO, et al. Self-organization of rat cardiac cells into contractile 3-D cardiac tissue. FASEB J 2005;19:275–7.
16. Okano T, Yamada N, Sakai H, Sakurai Y. A novel recovery system for cultured cells using plasma-treated polystyrene dishes grafted with poly(N-isopropylacrylamide). J Biomed Mater Res 1993;27:1243–51.
17. Miyagawa S, Sawa Y, Sakakida S, et al. Tissue cardiomyoplasty using bioengineered contractile cardiomyocyte sheets to repair damaged myocardium: their integration with recipient myocardium. Transplantation 2005;80:1586–95.
18. Nishida K, Yamato M, Hayashida Y, et al. Corneal reconstruction with tissue-engineered cell sheets composed of autologous oral mucosal epithelium. N Engl J Med 2004;351: 1187–96.
19. Kushida A, Yamato M, Isoi Y, Kikuchi A, Okano T. A noninvasive transfer system for polarized renal tubule epithelial cell sheets using temperature-responsive culture dishes. Eur Cell Mater 2005;10:23–9; discussion 30.
20. Masuda S, Shimizu T, Yamato M, Okano T. Cell sheet engineering for heart tissue repair. Adv Drug Deliv Rev 2008;60:277–85.
21. Kushida A, Yamato M, Konno C, et al. Decrease in culture temperature releases monolayer endothelial cell sheets together with deposited fibronectin matrix from temperature-responsive culture surfaces. J Biomed Mater Res 1999;45: 355–62.
22. Shimizu T, Yamato M, Kikuchi A, Okano T. Two-dimensional manipulation of cardiac myocyte sheets utilizing temperature-responsive culture dishes augments the pulsatile amplitude. Tissue Eng 2001;7:141–51.
23. Shimizu T, Yamato M, Akutsu T, et al. Electrically communicating three-dimensional cardiac tissue mimic fabricated by layered cultured cardiomyocyte sheets. J Biomed Mater Res 2002;60:110–7.
24. Shimizu T, Yamato M, Isoi Y, et al. Fabrication of pulsatile cardiac tissue grafts using a novel 3-dimensional cell sheet manipulation technique and temperature-responsive cell culture surfaces. Circ Res 2002;90:e40.
25. Shimizu T, Sekine H, Isoi Y, et al. Long-term survival and growth of pulsatile myocardial tissue grafts engineered by the layering of cardiomyocyte sheets. Tissue Eng 2006;12: 499–507.
26. Kubo H, Shimizu T, Yamato M, Fujimoto T, Okano T. Creation of myocardial tubes using cardiomyocyte sheets and an in vitro cell sheet-wrapping device. Biomaterials 2007;28:3508–16.
27. Sekine H, Shimizu T, Yang J, Kobayashi E, Okano T. Pulsatile myocardial tubes fabricated with cell sheet engineering. Circulation 2006;114:I87–93.
28. Haraguchi Y, Shimizu T, Yamato M, Kikuchi A, Okano T. Electrical coupling of cardiomyocyte sheets occurs rapidly via functional gap junction formation. Biomaterials 2006;27: 4765–74.
29. Furuta A, Miyoshi S, Itabashi Y, et al. Pulsatile cardiac tissue grafts using a novel three-dimensional cell sheet manipulation technique functionally integrates with the host heart, in vivo. Circ Res 2006;98:705–12.
30. Sekine H, Shimizu T, Kosaka S, Kobayashi E, Okano T. Cardiomyocyte bridging between hearts and bioengineered myocardial tissues with mesenchymal transition of mesothelial cells. J Heart Lung Transplant 2006;25:324–32.
31. Shimizu T, Sekine H, Yang J, et al. Polysurgery of cell sheet grafts overcomes diffusion limits to produce thick, vascularized myocardial tissues. FASEB J 2006;20:708–10.
32. Sekiya S, Shimizu T, Yamato M, Kikuchi A, Okano T. Bioengineered cardiac cell sheet grafts have intrinsic angiogenic potential. Biochem Biophys Res Commun 2006;341: 573–82.
33. Miyagawa S, Sawa Y, Taketani S, et al. Myocardial regeneration therapy for heart failure: hepatocyte growth factor enhances the effect of cellular cardiomyoplasty. Circulation 2002;105:2556–61.
34. Sekine H, Shimizu T, Hobo K, et al. Endothelial cell coculture within tissue-engineered cardiomyocyte sheets enhances neovascularization and improves cardiac function of ischemic hearts. Circulation 2008;118:S145–52.
35. Dib N, Michler RE, Pagani FD, et al. Safety and feasibility of autologous myoblast transplantation in patients with ischemic cardiomyopathy: four-year follow-up. Circulation 2005; 112:1748–55.
36. Memon IA, Sawa Y, Fukushima N, et al. Repair of impaired myocardium by means of implantation of engineered autologous myoblast sheets. J Thorac Cardiovasc Surg 2005;130: 1333–41.
37. Kondoh H, Sawa Y, Miyagawa S, et al. Longer preservation of cardiac performance by sheet-shaped myoblast implantation in dilated cardiomyopathic hamsters. Cardiovasc Res 2006;69:466–75.
38. Hata H, Matsumiya G, Miyagawa S, et al. Grafted skeletal myoblast sheets attenuate myocardial remodeling in pacing-induced canine heart failure model. J Thorac Cardiovasc Surg 2006;132:918–24.
39. Miyagawa S, Saito A, Sakaguchi T, et al. Impaired myocardium regeneration with skeletal cell sheets-a preclinical trial for tissue-engineered regeneration therapy. Transplantation 2010;90:364–72.
40. Itabashi Y, Miyoshi S, Yuasa S, et al. Analysis of the electrophysiological properties and arrhythmias in directly contacted skeletal and cardiac muscle cell sheets. Cardiovasc Res 2005;67:561–70.
41. Leobon B, Garcin I, Menasche P, et al. Myoblasts transplanted into rat infarcted myocardium are functionally isolated from their host. Proc Natl Acad Sci U S A 2003;100: 7808–11.
42. Hoashi T, Matsumiya G, Miyagawa S, et al. Skeletal myoblast sheet transplantation improves the diastolic function of a pressure-overloaded right heart. J Thorac Cardiovasc Surg 2009;138:460–7.
43. Miyahara Y, Nagaya N, Kataoka M, et al. Monolayered mesenchymal stem cells repair scarred myocardium after myocardial infarction. Nat Med 2006;12:459–65.
44. Hobo K, Shimizu T, Sekine H, et al. Therapeutic angiogenesis using tissue engineered human smooth muscle cell sheets. Arterioscler Thromb Vasc Biol 2008;28:637–43.
45. Kobayashi H, Shimizu T, Yamato M, et al. Fibroblast sheets co-cultured with endothelial progenitor cells improve cardiac function of infarcted hearts. J Artif Organs 2008;11: 141–7.
46. Sabbah HN. The cardiac support device and the myosplint: treating heart failure by targeting left ventricular size and shape. Ann Thorac Surg 2003;75:S13–9.
47. Memon IA, Sawa Y, Miyagawa S, Taketani S, Matsuda H. Combined autologous cellular cardiomyoplasty with skeletal myoblasts and bone marrow cells in canine hearts for ischemic cardiomyopathy. J Thorac Cardiovasc Surg 2005; 130:646–53.
48. Laflamme MA, Murry CE. Regenerating the heart. Nat Biotechnol 2005;23:845–56.
49. Jellis C, Martin J, Narula J, Marwick TH. Assessment of nonischemic myocardial fibrosis. J Am Coll Cardiol;56:89–97.
50. Leor J, Aboulafia-Etzion S, Dar A, et al. Bioengineered cardiac grafts: A new approach to repair the infarcted myocardium? Circulation 2000;102:III56–61.
51. Li RK, Jia ZQ, Weisel RD, et al. Survival and function of bioengineered cardiac grafts. Circulation 1999;100:II63–9.
52. Eschenhagen T, Fink C, Remmers U, et al. Three-dimensional reconstitution of embryonic cardiomyocytes in a collagen matrix: a new heart muscle model system. FASEB J 1997;11:683–94.
53. Zimmermann WH, Fink C, Kralisch D, et al. Three-dimensional engineered heart tissue from neonatal rat cardiac myocytes. Biotechnol Bioeng 2000;68:106–14.
54. Zimmermann WH, Schneiderbanger K, Schubert P, et al. Tissue engineering of a differentiated cardiac muscle construct. Circ Res 2002;90:223–30.

55. Zimmermann WH, Didie M, Wasmeier GH, et al. Cardiac grafting of engineered heart tissue in syngenic rats. Circulation 2002;106:I151–7.
56. Zimmermann WH, Melnychenko I, Wasmeier G, et al. Engineered heart tissue grafts improve systolic and diastolic function in infarcted rat hearts. Nat Med 2006;12:452–8.
57. Yildirim Y, Naito H, Didie M, et al. Development of a biological ventricular assist device: preliminary data from a small animal model. Circulation 2007;116:I16–23.
58. Naito H, Melnychenko I, Didie M, et al. Optimizing engineered heart tissue for therapeutic applications as surrogate heart muscle. Circulation 2006;114:I72–8.
59. Birla RK, Borschel GH, Dennis RG, Brown DL. Myocardial engineering in vivo: formation and characterization of contractile, vascularized three-dimensional cardiac tissue. Tissue Eng 2005;11:803–13.
60. Ozawa T, Mickle DA, Weisel RD, et al. Optimal biomaterial for creation of autologous cardiac grafts. Circulation 2002; 106:I176–82.
61. Giraud MN, Armbruster C, Carrel T, Tevaearai HT. Current state of the art in myocardial tissue engineering. Tissue Eng 2007;13:1825–36.
62. McDevitt TC, Woodhouse KA, Hauschka SD, Murry CE, Stayton PS. Spatially organized layers of cardiomyocytes on biodegradable polyurethane films for myocardial repair. J Biomed Mater Res A 2003;66:586–95.
63. Jawad H, Lyon AR, Harding SE, Ali NN, Boccaccini AR. Myocardial tissue engineering. Br Med Bull 2008;87:31–47.
64. Lobler M, Sass M, Kunze C, Schmitz KP, Hopt UT. Biomaterial implants induce the inflammation marker CRP at the site of implantation. J Biomed Mater Res 2002;61:165–7.
65. Ott HC, Matthiesen TS, Goh SK, et al. Perfusion-decellularized matrix: using nature's platform to engineer a bioartificial heart. Nat Med 2008;14:213–21.
66. Akhyari P, Fedak PW, Weisel RD, et al. Mechanical stretch regimen enhances the formation of bioengineered autologous cardiac muscle grafts. Circulation 2002;106:I137–42.
67. Kofidis T, Akhyari P, Boublik J, et al. In vitro engineering of heart muscle: artificial myocardial tissue. J Thorac Cardiovasc Surg 2002;124:63–9.
68. Xiang Z, Liao R, Kelly MS, Spector M. Collagen-GAG scaffolds grafted onto myocardial infarcts in a rat model: a delivery vehicle for mesenchymal stem cells. Tissue Eng 2006;12:2467–78.
69. Simpson D, Liu H, Fan TH, Nerem R, Dudley SC, Jr. A tissue engineering approach to progenitor cell delivery results in significant cell engraftment and improved myocardial remodeling. Stem Cells 2007;25:2350–7.
70. Matsubayashi K, Fedak PW, Mickle DA, et al. Improved left ventricular aneurysm repair with bioengineered vascular smooth muscle grafts. Circulation 2003;108(suppl 1):II219–25.
71. Fukuhara S, Tomita S, Nakatani T, et al. Bone marrow cell-seeded biodegradable polymeric scaffold enhances angiogenesis and improves function of the infarcted heart. Circ J 2005;69:850–7.
72. Kellar RS, Landeen LK, Shepherd BR, et al. Scaffold-based three-dimensional human fibroblast culture provides a structural matrix that supports angiogenesis in infarcted heart tissue. Circulation 2001;104:2063–8.
73. Kellar RS, Shepherd BR, Larson DF, Naughton GK, Williams SK. Cardiac patch constructed from human fibroblasts attenuates reduction in cardiac function after acute infarct. Tissue Eng 2005;11:1678–87.
74. Chachques JC, Trainini JC, Lago N, et al. Myocardial Assistance by Grafting a New Bioartificial Upgraded Myocardium (MAGNUM trial): clinical feasibility study. Ann Thorac Surg 2008;85:901–8.
75. Oh H, Bradfute SB, Gallardo TD, et al. Cardiac progenitor cells from adult myocardium: homing, differentiation, and fusion after infarction. Proc Natl Acad Sci U S A 2003;100: 12313–8.
76. Beltrami AP, Barlucchi L, Torella D, et al. Adult cardiac stem cells are multipotent and support myocardial regeneration. Cell 2003;114:763–76.
77. Matsuura K, Nagai T, Nishigaki N, et al. Adult cardiac Sca-1-positive cells differentiate into beating cardiomyocytes. J Biol Chem 2004;279:11384–91.
78. Gaballa MA, Sunkomat JN, Thai H, et al. Grafting an acellular 3-dimensional collagen scaffold onto a nontransmural infarcted myocardium induces neo-angiogenesis and reduces cardiac remodeling. J Heart Lung Transplant 2006;25:946–54.
79. Fujimoto KL, Tobita K, Merryman WD, et al. An elastic, biodegradable cardiac patch induces contractile smooth muscle and improves cardiac remodeling and function in subacute myocardial infarction. J Am Coll Cardiol 2007;49: 2292–300.
80. Callegari A, Bollini S, Iop L, et al. Neovascularization induced by porous collagen scaffold implanted on intact and cryoinjured rat hearts. Biomaterials 2007;28:5449–61.
81. Ota T, Gilbert TW, Badylak SF, Schwartzman D, Zenati MA. Electromechanical characterization of a tissue-engineered myocardial patch derived from extracellular matrix. J Thorac Cardiovasc Surg 2007;133:979–85.
82. Badylak SF, Kochupura PV, Cohen IS, et al. The use of extracellular matrix as an inductive scaffold for the partial replacement of functional myocardium. Cell Transplant 2006;15(suppl 1):S29–40.
83. Robinson KA, Li J, Mathison M, et al. Extracellular matrix scaffold for cardiac repair. Circulation 2005;112:I135–43.
84. Kochupura PV, Azeloglu EU, Kelly DJ, et al. Tissue-engineered myocardial patch derived from extracellular matrix provides regional mechanical function. Circulation 2005; 112:I144–9.
85. Chang Y, Chen SC, Wei HJ, et al. Tissue regeneration observed in a porous acellular bovine pericardium used to repair a myocardial defect in the right ventricle of a rat model. J Thorac Cardiovasc Surg 2005;130:705–11.

Adipose Tissue-Derived Multi-lineage Progenitor Cells as a Promising Tool for *In Situ* Stem Cell Therapy

Hanayuki Okura[1], Ayami Saga[1], Mayumi Soeda[1], Akihiro Ichinose[2] and Akifumi Matsuyama[1,3,*]

[1]*Department of Somatic Stem Cell Therapy and Health Policy, Foundation for Biomedical Research and Innovation, 2-2 Minatojima-minamimachi, Chuo-ku, Kobe, 650-0047, Japan*

[2]*Department of Plastic Surgery, Kobe University Hospital, 7-5-2 Kusunoki-cho, Chuo-ku, Kobe, Hyogo, 650-0017, Japan*

[3]*The Center for Medical Engineering and Informatics, Osaka University, 2-2 Yamada-oka, Suita, Osaka, 565-0871, Japan*

Abstract: Adipose tissue-derived cell sources are attractive for regenerative medicine due to the easy and safe accessibility of adipose tissue, lack of ethical issues, and their availability in large quantities. We have developed an isolation method for distinct stem cells, and named the cells adipose tissue-derived multilineage progenitor cells (ADMPC). ADMPC have higher potential for differentiation into adipocytic, osteocytic, and chondrocytic progeny than the widely reported adipose tissue-derived stromal/stem cells (ADSC). ADMPC can also differentiate into hepatocyte-like clusters *in vitro* by induction with the hepatogenic cytokines, hepatocyte growth factor, oncostatin M, and basic fibroblast growth factor. *In vivo*, ADMPC were reprogrammed *in situ* into hepatocyte-like cells that corrected the metabolic defect in hyperlipidemic Watanabe rabbits after transplantation *via* the portal vein. Such cells are potentially useful in regenerative medicine as sources for *in situ* stem cell therapy.

Keywords: adipose tissue, ADMPC, *in situ* stem cell therapy, *in situ* reprogramming, *in situ* differentiation, ADSC, ADMSC, ASC.

1. INTRODUCTION

The recent finding of differentiation-capable adult somatic stem cells holds great promise for regenerative medicine [1]. Extensive research is also ongoing into mesenchymal stem cells (MSC), found in human bone marrow, scalp tissue, placenta, umbilical cord matrix, and various fetal tissues [2-6]. Among these MSC sources, adipose tissue is particularly attractive for regenerative medicine because the tissues can be easily and safely accessed, are free of any ethical issues, and are available in large amounts. Many investigators have also reported that the cells derived from adipose tissue (adipose tissue-derived stromal/stem cells [ADSC], also referred to as adipose tissue-derived mesenchymal stem cells [ADMSC]) could differentiate into various cell types *in vitro* including chondrocytes, osteoblasts, adipocytes, myocytes, neuronal cells, and hepatocytes [1-4]. ADSC are considered as a colony-forming cell-rich fraction of adherent cells, which can attach to plastic culture dishes after isolation of the stromal vascular fraction (SVF), and thereafter be expanded and maintained in monolayer cultures as a heterogeneous population [7]. However, although ADSC can differentiate into various cell types *in vitro*, their self-renewal potency decreases significantly with passaging making them unsuitable for regenerative medicine applications.

*Address correspondence to this author at the Department of Somatic Stem Cell Therapy and Health Policy, Foundation for Biomedical Research and Innovation, 2-2 Minatojima-minamimachi, Chuo-ku, Kobe, 650-0047, Japan; Tel: +81-78-304-8706; Fax: +81-78-304-8707;
E-mail: akifumi-matsuyama@umin.ac.jp

In this review, we describe a novel population of adipose tissue-derived stem cells with higher differentiation potential than other well-reported adipose tissue-derived cells; we named these adipose tissue-derived multi-lineage progenitor cells (ADMPC). ADMPC could differentiate into hepatocyte-like cells *in vitro*, and in the hepatic environment *in vivo*. These *in situ* reprogrammed cells successfully corrected the metabolic defect in diseased animals, indicating that such *in situ* reprogramming could be applied for regenerative medicine as "*in situ* stem cell therapy".

2. MATERIALS AND METHODS

2.1. Adipose Tissues

Adipose tissues were resected from five human subjects as excess discards during plastic surgery (females, age, 20-60 years). Ten to fifty grams of subcutaneous adipose tissue were collected from each subject. All subjects provided informed consent and the Review Board for Human Research of Kobe University Graduate School of Medicine and Foundation for Biomedical Research and Innovation approved the study protocol.

2.2. Isolation of ADMPC

Human ADMPC (hADMPC) were prepared as described previously [8-13]. Briefly, the resected adipose tissue was minced and then digested at 37°C for 1 h in Hank's balanced salt solution (HBSS, GIBCO Invitrogen, Grand Island, NY) containing 0.075% collagenase type II (Sigma Aldrich, St. Louis, MO). Digests were filtered through a cell strainer (BD Bioscience, San Jose, CA) and centrifuged at 800 x *g* for 10

2211-5420/12 $58.00+.00

min. Red blood cells were excluded using density gradient centrifugation with Lymphoprep (d = 1.077; Nacalai Tesque, Kyoto, Japan), and the remaining cells were cultured in Dulbecco's modified Eagle's medium (DMEM, GIBCO Invitrogen) with 10% defined fetal bovine serum (FBS, GIBCO Invitrogen) for 24 h at 37°C. Following incubation, the adherent cells were washed extensively and then treated with 0.2 g/l ethylenediaminetetraacetate (EDTA) solution (Nacalai Tesque). The resulting suspended cells were replated at a density of 10,000 cells/cm^2 on human fibronectin (FN)-coated dishes (AGC, Tokyo, Japan) in Stem Cell Medium (Nipro, Osaka, Japan) containing 1 x insulin-transferrin selenium (ITS, GIBCO Invitrogen.), 1 nM dexamethasone (Sigma Aldrich), 100 μM ascorbic acid 2-phosphate (Sigma Aldrich), 10 ng/ml epidermal growth factor (EGF, PeproTec, Rocky Hill, NJ), and 5% FBS. After passaging 5 to 6 times in the same medium, the ADMPC were ready for use in experiments. ADSC were isolated and cultured as reported by Zuk *et al.* [7].

2.3. Adipocytic, Osteocytic, and Chondrocytic Differentiation Procedure

For adipocytic differentiation, cells were cultured in Differentiation Medium (Zen-Bio, Research Triangle Park, NC) [14]. After three days, half of the medium was replaced with Adipocyte Medium (Zen-Bio) and this was repeated every two days. Five days after differentiation, adipocytes were identified by intracellular lipid droplets observed microscopically after Oil Red O staining. In brief, cultures were fixed in Baker's formal calcium, washed in 60% isopropanol, and stained with double-filtered Oil Red O solution to identify lipid accumulation. To determine the lipid content, Oil-Red O was extracted from the differentiated cells with isopropanol and absorbance of the contents was evaluated. Osteocytic differentiation was induced by culturing the cells in DMEM containing 10 nM dexamethasone, 50 mg/dl ascorbic acid 2-phosphate, 10 mM beta-glycerophosphate (Sigma Aldrich), and 10% FBS. Differentiation was evaluated by Alizarin red staining and alkaline phosphatase (ALPase) activity as described previously [15]. For Alizarin red staining, the cells were washed three times and fixed with dehydrated ethanol. After fixation, the cells were stained with 1% Alizarin red S in 0.1% NH_4OH (ph 6.5) for 5 minutes, and then washed with H_2O. ALPase activity per cell was calculated based on the amount of DNA. For chondrocytic differentiation, ADMPC were trypsinized and 2 x 10^5 cells were centrifuged at 400 x *g* for 10 minutes. The resulting pellets were cultured in chondrogenic medium (α-MEM supplemented with 10 ng/ml transforming growth factor (TGF)-β, 10 nM dexamethasone, 100 μM ascorbate, and 10 μl/ml 100 x ITS Solution) for 14 days [8]. The osteogenic differentiation was assessed by Alcian Blue staining, whereby nuclear counterstaining with Weigert's hematoxylin was followed by 0.5% Alcian Blue 8GX, which binds proteoglycan-rich cartilage matrix.

2.4. Differentiation of Hepatocyte-Like Cell Clusters

The differentiation procedure consisted of three stages. In stage I, ADMSC were cultured and expanded in medium I for three to four passages. In stage II, the cells were dissociated with trypsin-EDTA and the resulting single cells were suspended in medium II (80% knockout-DMEM [GIBCO Invitrogen], 20% defined FBS, 1 mM glutamine, and 1% nonessential amino acids [both from GIBCO Invitrogen]). The suspension was placed in an ultralow-attachment culture dish (Hydrocell; CellSeed, Tokyo, Japan), and the cells self-aggregated into cell clusters within 1 day. The cell clusters were then cultured for an additional 2 days. In stage III, after washing extensively with PBS, 2-day-old cell clusters (average of 1000 cells each) were cultured on a Hydrocell dish for 4 weeks in medium III (60% DMEM-low glucose, 40% MCDB-201, 1 nM dexamethasone, 100 mM ascorbic acid, 10 ng/ml EGF, basic fibroblast growth factor [bFGF, Peprotech, Rocky Hill, NJ], hepatocyte growth factor [HGF, Peprotech], and oncostatin M [OSM]). Finally, 0.1% dimethyl sulfoxide (DMSO; Nacalai Tesque) was added on the 10th day after induction of differentiation.

2.5. DiO or DiI Labeling of LDL

Human LDL (density 1.019-1.063 g/ml) was isolated by sequential ultracentrifugation from normolipidemic donors, dialyzed against saline-EDTA, and then sterilized by filtration through a 0.2-μm filter. Lipoproteins were labeled with DiO or DiI (Sigma) by incubating the LDL in 0.5% bovine serum albumin (BSA)/PBS with 100 ml DiO or DiI in DMSO (3 mg/ml) for 8 h at 37°C. The lipoproteins were then dialyzed against PBS and filtered before use.

2.6. Cell Transplantation and Immunosuppression

The protocols for cell transplantation and immunosuppression were described previously [12]. In brief, WHHL rabbits (8-week-old, purchased from Kitayamalabes, Ina, Nagano, Japan) were anesthetized with 50 mg/kg pentobarbital. An incision distal and parallel to the lower end of the ribcage was made, followed by a peritoneal incision and infusion of the ADMPC or control into the portal vein. The immunosuppression regimen consisted of the following: i) intramuscular injection of 6 mg/kg/day cyclosporin A daily from the day before surgery to sacrifice, ii) intramuscular injection of 0.05 mg/kg/day rapamycin daily from the day before surgery to sacrifice, iii) methylprednisolone at 3 mg/kg/day (day -1 to 7), followed by tapering to 2 mg/kg/day (day 8 to 14), 1 mg/kg/day (day 15 to 21), and 0.5 mg/kg/day (day 22 to the time at sacrifice), iv) intravenous injection of 20 mg/kg/day cyclophosphamide at days 0, 2, 5, and 7, and, v) intramuscular injection of 2.5 mg/kg/day ganciclovir to avoid viral infection in the immunocompromised host.

2.7. Immunohistochemical Staining of WHHL Rabbit Liver Sections

The WHHL livers were harvested and fixed immediately with 10% formalin. They were placed into optimal cutting temperature (OCT) compound (Sakura Finetechnical), frozen immediately, and then sectioned at 7 μm-thickness. The sections were incubated with blocking solution (Blocking one; Nacalai Tesque) for 1 h, and then incubated with rabbit anti-human albumin antibody (MBL, Nagoya, Japan) or mouse anti-human CD90 antibody followed by Alexa Fluor 488-labeled goat anti-rabbit IgG or Alexa Fluor 546-labeled goat anti-mouse IgG (Molecular Probes, Eugene, OR). The stained sections were examined with a BioZero laser scanning microscope (Keyence, Osaka, Japan).

Table 1. Differences Between ADMPC and ADSC of their Differentiation / Proliferation Abilities

	Self-Aggregation Properties	EDTA-Sensitiveness	Differentiation Abilities			Proliferation Abilities	
			Adipocytic	Osteocytic	Chondrocytic	After Reseeding	After ßPassaging
ADMPC	+	+	++	++	++	+	++
ADSC	-	-	+	+	+	++	++

2.8. PCR Analysis of WHHL Rabbit Liver for Human Liver-Specific Genes

Total RNAs of WHHL rabbit liver, hADMPC, and human hepatocytes were isolated using an RNAeasy kit (Qiagen, Valencia, CA). After treatment with DNase, the cDNAs were synthesized using Superscript III RNase H-minus Reverse Transcriptase (Invitrogen). Real-time PCR was performed using the ABI Prism 7900 Sequence Detection System (Applied Biosystems, Foster City, CA). 20X Assays-on-Demand™ Gene Expression Assay Mix for human alpha-1-antitrypsin (hAAT1) (Hs01097800_m1), human albumin (Hs00609411_m1), human Factor 9, human GATA4 (Hs00171403_m1), human hepatocyte nuclear factor 3beta (HNF-3beta) (Hs00232764_m1), human LDL receptor (Hs00181192_m1), and human glyceraldehyde-3-phosphate dehydrogenase (GAPDH) (Hs99999905_m1) were obtained from Applied Biosystems. It was confirmed that our human detectors and rabbit detectors did not cross-react with the other species. TaqMan® Universal PCR Master Mix and No AmpErase® UNG (2X) were also purchased from Applied Biosystems. Reactions were performed in quadruplicate and the mRNA levels were normalized relative to human GAPDH expression. To confirm that hADMPC differentiated into hepatocytes *in vivo*, the cells were tested by quantitative PCR before transplantation using human primary hepatocytes (Invitrogen, Lot number; HuP81) as controls.

2.9. Assay for Lipid Profiling

Serum samples were obtained from nonfasting rabbits before and after transplantation. Serum total cholesterol was measured in each sample using assay kits from Wako Pure Chemical Industries (Osaka, Japan). Serum lipoproteins were analyzed by an on-line dual enzymatic method for simultaneous quantification of cholesterol and triglycerides by high-performance liquid chromatography at Skylight Biotech (Akita, Japan), according to the described procedure [21].

2.10. Clearance of ^{125}I-LDL from Rabbit Serum

WHHL rabbits (8 weeks old) were anesthetized with pentobarbital (50 mg/kg). The peritoneum was incised and hADMPC (high-dose; 3 x 10^7 cells/rabbit, n = 2, low-dose; 5 x 10^6 cells/rabbit, n = 2) suspended in 3 ml of HBSS (20°C) (n = 5) or 3 ml of control (n = 2) were infused into the portal vein via an 18-gauge Angiocath™ (BD, UT). Eight weeks later, the animals were tested by the LDL turnover assay. ^{125}I-labeled human LDL (BT-913R, Biomedical Technologies, Stoughton, MA) was delivered via the marginal ear vein of the WHHL rabbits. Blood was collected from the opposite ear after injection at 5 min, 1 h, 2 h, 4 h, 6 h, and 28 h. ^{125}I-labeled apolipoprotein B-containing LDL was precipitated with 20% trichloroacetic acid (Wako Pure Chemical Industries) (serum; 320 µl, 100% w/v TCA 80 µl), and then the precipitants were applied for counting.

2.11. Statistical Analysis and Ethical Considerations

All animal studies described in this report were approved by Kobe University Graduate School of Medicine and Foundation for Biomedical Research and Innovation. Values were expressed as mean ± SEM. Differences between mean values of treated and untreated groups were evaluated using the Student's t-test. A P value less than 0.05 was considered statistically significant. All statistical analyses were performed using the SPSS Statistics 17.0 package (SPSS Inc., Chicago, IL).

3. RESULTS AND DISCUSSION

3.1. Self-Aggregation Properties and EDTA-Sensitivity of ADMPC

In the ADMPC isolation procedure were shown in Fig. (**1A**) (cited from reference 12 with modification). First, we removed contaminating red blood cells using density gradient centrifugation after digestion of adipose tissue to obtain the stromal vascular fraction (SVF). After 24-hour culture of the SVF (Fig. **1Aa**), adherent cells were treated with EDTA solution and the suspended cells were collected. Finally, these cells were re-plated on human FN-coated dishes (Fig. **1Ab**) and cultured (Fig. **1Ac**). Within 2–3 passages after the initial plating of the primary culture, ADMPC appeared as a monolayer of large flat cells (25–30 µm in diameter). As the cells approached confluence, they became spindle-shaped, resembling fibroblasts (Fig. **1Ad**). We next analyzed the mRNA expression levels of *islet-1* and *nkx2.5* in the two types of cells. *Islet-1* is a marker of undifferentiated cells and progenitors of cardiomyocytes, hepatocytes and pancreatic β cells, and *nkx2.5* is a marker of progenitors of cardiomyocytes. As shown in Fig. (**1B**), *islet-1* and *nkx2.5* were expressed in ADMPC, but not in ADSC. No or faint staining was noted for *GATA-4*, *myosin light chain*, *alpha cardiac actin*, and *myosin heavy chain* expression in both ADMPC and ADSC. On the other hand, flowcytometric analysis showed no significant different pattern in their cell surface markers between ADMPC and ADSC.

3.2. Adipocytic, Osteocytic and Chondrocytic Differentiation

In the next step, we assessed whether the adipocytic, osteocytic, and chondrocytic differentiation potentials of ADMPC were higher than those of ADSC (Table **1**). Adipo-

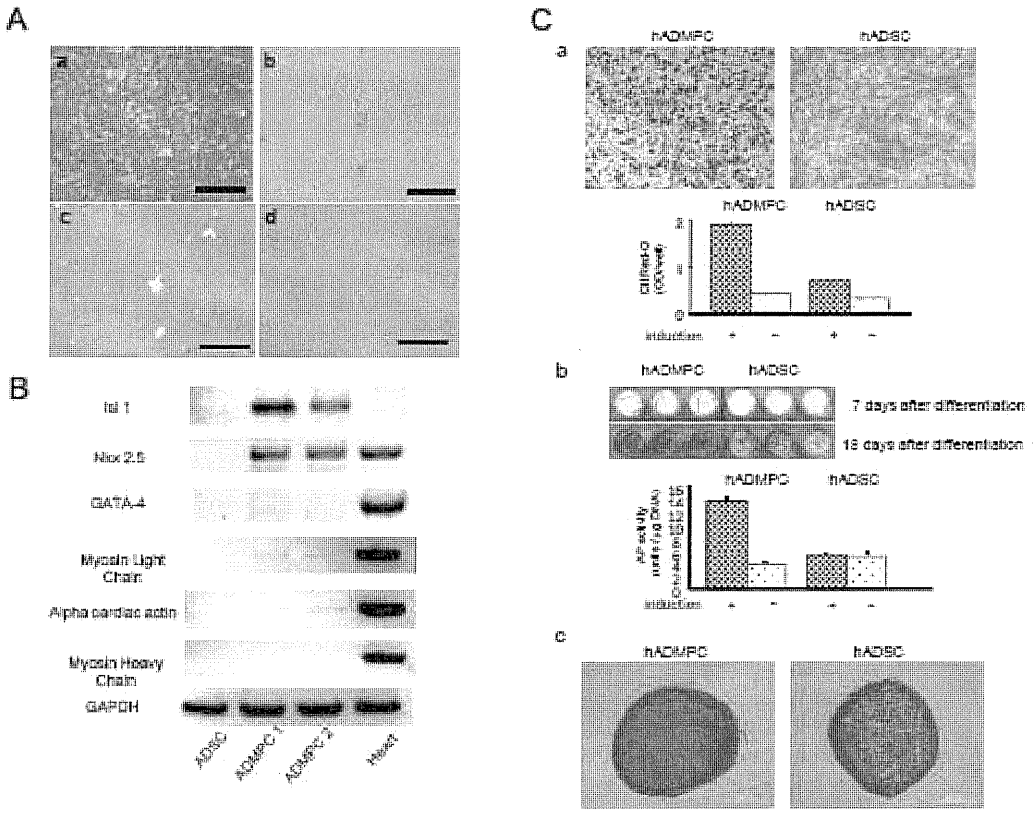

Fig. (1). Characters of ADMPC (**A**) Morphological characteristics of ADMPC. The cells obtained from adipose tissue were seeded and incubated for 24 h (a). Following incubation, the adherent cells were treated with EDTA solution, and the resulting suspended cells were replated at a density of 10,000 cells/cm^2 on human fibronectin (FN)-coated dishes (BD BioCoat) (b and c). Within 2–3 passages after the initial plating of the primary culture, ADMPC appeared as a monolayer of large flat cells (25–30 μm in diameter). As the cells approached confluence, they assumed a more spindle-shaped, fibroblastic morphology (d). Calibration bars = 500 μm (a, c and d) and 200 μm (b). Cited from reference 12 with modification. (**B**) Comparison of mRNA expression of markers of undifferentiated cells on ADMPC and ADSC. Islet-1, a marker of undifferentiated cells and progenitors of cardiomyocytes, hepatocytes, and pancreatic β cells, and nkx2.5, a transcription factor known to mark cardiomyocyte differentiation, were expressed in ADMPC, but not ADSC. GATA-4, a myosin light chain protein, α-cardiac actin, and myosin heavy chain protein were absent or only faintly stained in both cell types. Human heart mRNA was used as the control in these experiments. (**C**) Differences in the differentiation potentials between ADMPC and ADSC. (a) Morphological comparison of the adipogenic differentiation potential of ADMPC and ADSC. The cells were cultured in Differentiation Medium. After three days, half of the medium was replaced with adipocyte medium and this was repeated every two days. Five days after differentiation, the lipid contents of differentiated adipocytes were confirmed by Oil Red O staining. The lipid contents of differentiated adipocytes were confirmed by Oil Red O extraction. hADMPC showed higher lipid contents than hADSC. Data are mean ± SEM of triplicate experiments. (b) Morphological comparison of osteogenic differentiation potential of ADMPC and ADSC. At 7 or 18 days after osteogenic differentiation, the cells were stained with Alizarin red S for mineralized nodules. ADMPC showed higher osteogenic differentiation potential than ADSC. even days after osteogenic differentiation, the cells were assayed for alkaline phosphatase (APase) activity. AP activity per cell was calculated based on the amount of DNA. hADMPC showed higher APase activity than hADSC. Data are mean ± SEM of triplicate experiments. (c) Comparison of chondrogenic differentiation potential between ADMPC and ADSC. Extracellular matrices of differentiated ADMPC and ADSC into chondrocytes were visualized with Alcian Blue staining.

cytic differentiation was induced by culture with the Differentiation Medium containing 1-methyl-3-isobutylxanthine, dexamethasone, and insulin. Induction was confirmed by the accumulation of intracellular lipid droplets that could be stained with Oil Red O. The results showed higher levels of adipocytic induction for ADMPC than ADSC (Fig. **1Ca**). Next, osteocytic induction was examined by Alizarin red S staining (Fig. **1Cb**). After a 7-day induction for osteocytic differentiation, ADMPC only were stained with Alizarin red S. ADSC were stained after an 18-day induction, but their staining intensity lagged behind that of ADMPC (Fig. **1Cb**). Third, the chondrocytic differentiation potential of ADMPC and ADSC was compared. As shown in Fig. (**1Cc**), ADMPC showed more intense Alcian Blue staining than ADSC, suggesting higher chondrocytic induction for ADMPC than ADSC. The self-aggregation properties of ADMPC might introduce their higher chondrocytic induction than ADSC. These results indicated that ADMPC have higher differentiation potentials than ADSC.

3.3. *In Vitro* Differentiation of ADMPC into Hepatocytes

To obtain hepatocyte-like cell clusters, we have established a three-step method (Fig. **2A**). Immunofluorescence staining (Fig. **2B**) showed albumin- and alpha-1-antitrypsin-expressing cells among the differentiated ADMPC (cited from reference 10 with modification). The ability to secrete

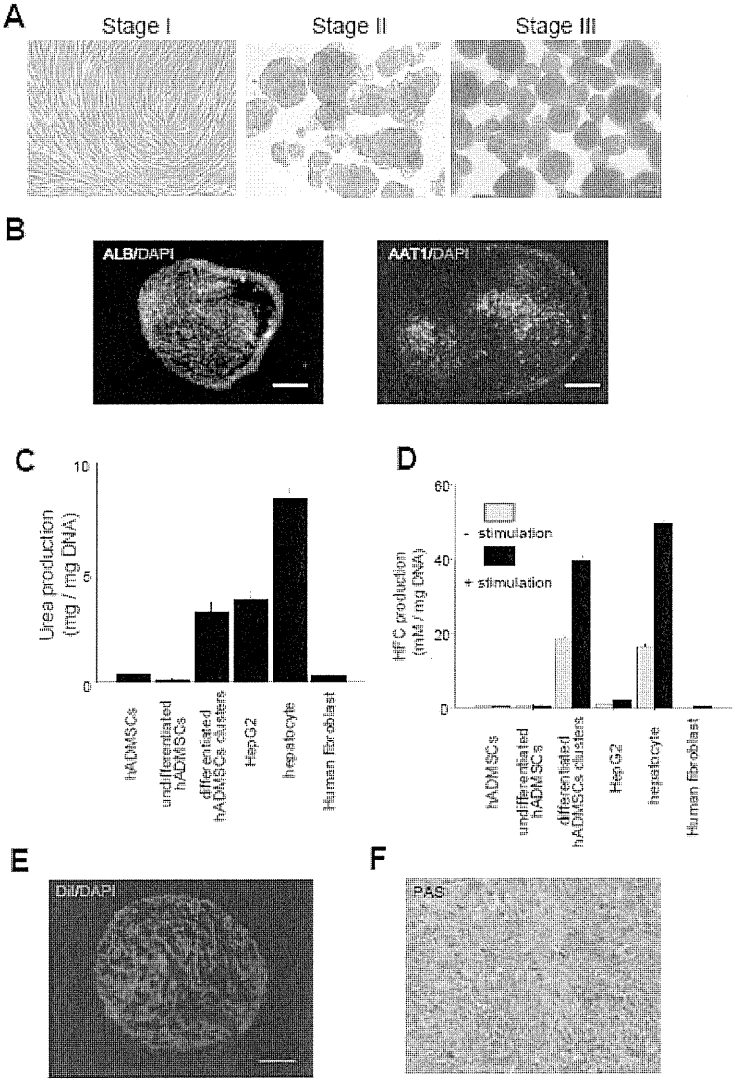

Fig (2). (**A**) General outline of the three-stage differentiation protocol. Stage I: growth of hADMSCs. Stage II: formation of cell clusters by culture in low osmotic medium on ultralow-attachment culture dishes. Stage III: growth factor stimulation of cell cluster cultures with bFGF, HGF, and OSM. DMSO was added on the 10th day after induction. (**B**) Immunofluorescence staining for ALB (left) and AAT (right) in differentiated ADMPC clusters. Scale bar, 100 mm. (**C**) Urea synthesis by differentiated ADMPC clusters after incubation with 5 mM NH_4Cl. Urea synthesis per cell was calculated based on the amount of DNA. Data are mean±SEM of triplicate experiments. (**D**) CYP enzyme activity in differentiated ADMPC clusters, as determined by hydroxylation of 7-benzyloxy-4-trifluoromethyo-coumarin to HFC. Before incubation with 100 mM, cells were cultured in the absence (non-stimulation) or presence (stimulation) of 10 mM rifampicin. CYP activity per cell was calculated based on the amount of DNA. Data are mean±SEM of triplicate experiments. (**E**) Low-density lipoprotein uptake by differentiated ADMPC clusters. Samples were examined by confocal laser scanning microscopy. Scale bar, 100 mm. (**F**) Glycogen storage in differentiated ADMPC clusters, as determined by PAS staining. hALB, human ALB; SEM, standard error of the mean; HFC, 7-hydroxy-4-trifluoromethyl-coumarin; PAS, periodic acid-Schiff's; DiI, 1,10-dioctadecyl-3,3,30,30-tetramethylindocarbocyanine; DAPI, 40,6-diamidino-2-phenylindole.

urea was about 12-fold higher for differentiated ADMPC incubated with NH_4Cl, compared with stage I undifferentiated ADMPC, and as high as that of HepG2 cells (Fig. **2C**). Nonfluorescent 7-benzyl-trifluoromethyl coumarin (BFC) is metabolized mainly by the cytochrome P450 (CYP) 3A family of enzymes and converted to the fluorescent 7-hydroxy-4-trifluoromethylcoumarin (HFC). The concentration of HFC in the supernatant was measured after incubation with 100 mM BFC. CYP activity in differentiated ADMPC clusters was 40-fold higher than in undifferentiated ADMPC (Fig. **2D**). In addition, CYP activity in differentiated ADMPC clusters increased 2–2.5-fold following preincubation with rifampicin for 3 days. In contrast, no increase in CYP activity was induced in undifferentiated ADMPC under this condition. We also assessed LDL uptake by differentiated ADMPC clusters by incubating differentiated ADMPC with DiI-LDL (Fig. **2E**). DiI-LDL was markedly incorporated into the cytosol of differentiated ADMPC. Another function of hepatocytes is glycogen production (glyconeogenesis), and PAS staining showed glycogen storage in differentiated ADMPC (Fig. **2F**). These results suggest that hepatogenic cytokines and floating culture could mimic the liver microenvironment and promote the differentiation of ADMPC into hepatocyte-like cells *in vitro*.

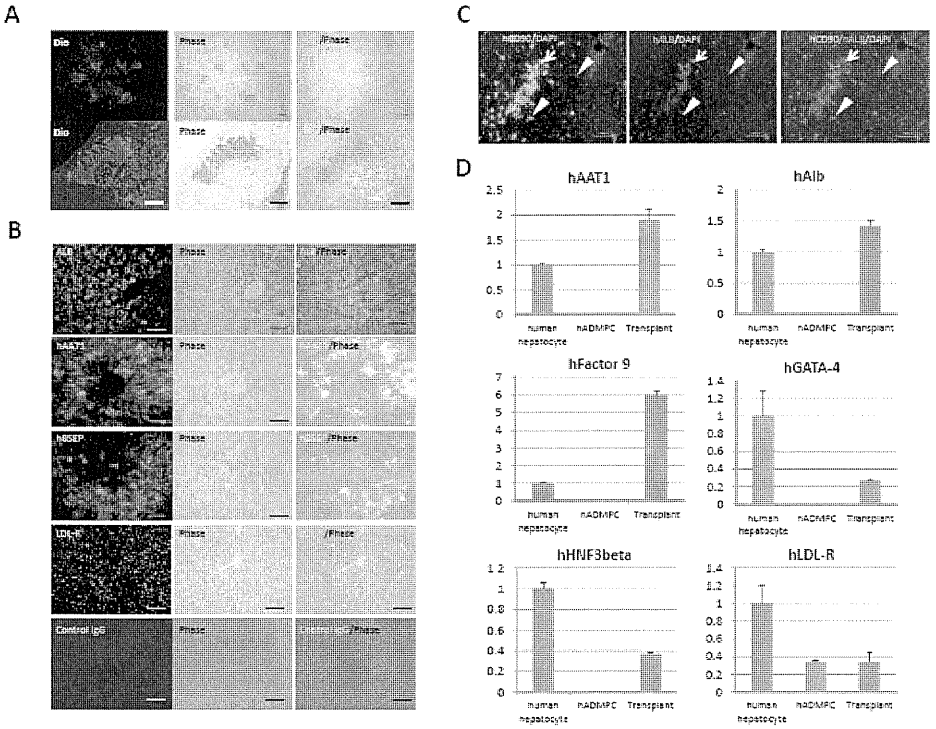

Fig (3). (A) Localization of transplanted hADMSCs in the WHHL liver. One week after transplantation of DiO-labeled hADMSCs via the portal vein, the WHHL rabbit liver was examined histologically. The DiO-labeled cells were localized in the portal area and dispersed in a centrilobular direction, resembling the mature innate hepatocytes. Bars = 200 μm (upper panels) and 100 μm (lower panels). **(B)** Immunohistochemical identification of human hepatocytic marker cells in liver sections of WHHL rabbits after ADMPC transplantation. Twelve weeks after ADMPC transplantation, human albumin-, human alpha-1-antitrypsin-, human bile salt export pump (BSEP)-, and LDL-receptor-positive cells were dispersed within the peri-venous regions of the liver parenchyma, where they made contact with and integrated among the host cells with cell-cell interactions between ADMPC-derived cells and diseased hepatocytes. Bar = 100 μm. **(C)** Differentiation of transplanted ADMPC into hepatocyte-like cells. Twelve weeks after transplantation, nearly all the human CD90-positive cells expressed human albumin, indicating that the major proportion of transplanted ADMPC could differentiate into hepatocyte-like cells (left panel: human CD90; middle panel: human albumin; right panel: merge). Arrows indicate human CD90 and human albumin double-positive cells; arrowheads indicate human CD90-positive/human albumin-negative cells. **(D)** Human hepatic gene expression in WHHL rabbit liver after ADMPC transplantation. RNA was prepared from WHHL rabbit livers 12 weeks after ADMPC transplantation. We examined expressions of the following hepatic markers by quantitative real time-polymerase chain reaction (RT-PCR) using the Assays-on-Demand Gene Expression Assay Mix: human alpha-1-antitrypsin, human albumin, human factor IX, human GATA-binding protein 4 (GATA-4), human hepatocyte nuclear factor 3 (HNF-3) beta, and human LDL-receptor. The livers of the control WHHL rabbits (saline, n = 3) were negative for all tested human hepatic genes. The mRNA levels were normalized based on human glyceraldehyde-3-phosphate dehydrogenase as a housekeeping gene and data are expressed as mean±SEM of triplicate experiments. The livers of ADMPC-recipient WHHL rabbits (n = 3) were positive for all tested human hepatic genes, which showed expression levels similar to those of human primary hepatocytes, but not ADMPC *per se*. Data are mean ± SEM.

3.4. in situ Reprogramming of ADMPC into Hepatocytes

One week after transplantation of hADMPC via the portal vein, we examined whether the cells reside or not in the liver after transplantation. As shown in Fig. (**3A**), DiO-fluorescent labeled-hADMPC resided and distributed in the portal area, and morphologically resembled innate hepatocytes. Next, we should examine the recruitment of these cells directly into the rabbit liver and the success of hepatocytic differentiation. For this purpose, we measured human-specific hepatocytic proteins and their hepatic functions (Fig. **3**, cited from reference 12 with modification). Human albumin-, alpha-1-antitrypsin-, bile salt export pump-, and LDL-receptor-positive cells were dispersed within peri-venous regions of the liver parenchyma, where they had contacted and integrated among the host cells (Fig. **3B**). We also identified conserved cell-cell interactions between ADMPC-derived and diseased hepatocytes. To confirm this finding and to assess the efficacy of differentiation, we colocalized human CD90 and human albumin. As shown in Fig. (**3C**), nearly all human CD90-positive cells expressed human albumin, indicating that about 80% or more of transplanted ADMPC differentiated into human albumin-positive hepatocyte-like cells at 12 weeks after transplantation. Next, to confirm the differentiation of ADMPC into hepatocytes *in vivo*, the expression of hepatocyte markers was analyzed by quantitative RT-PCR. WHHL rabbit liver that was transplanted with ADMPC expressed higher levels of human-specific alpha-1-antitrypsin, albumin, and coagulation factor IX than control ADMPC (Fig. **3D**). The expression levels of human GATA-4, human hepatocyte nuclear factor 3 beta, and LDL-receptor were also higher in the WHHL rabbit liver than in the ADMPC untransplanted liver (Fig. **3D**). These results verified that ADMPC *per se* could differentiate into mature hepatocytes *in vivo*.

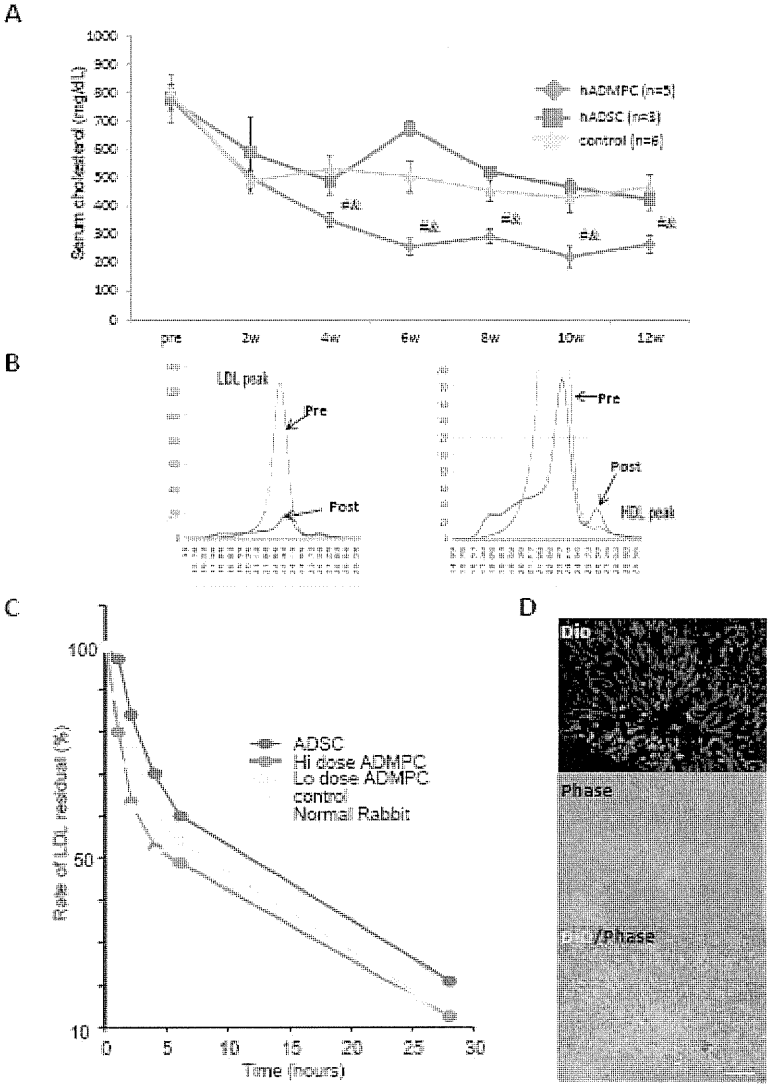

Fig. (4). (**A**) Total serum cholesterol levels. ADMPC transplantation in WHHL rabbits was followed for 12 weeks. Total serum cholesterol was measured in five rabbits that each received 3 x 10^7 ADMPC, three rabbits that each received 3 x 10^7 ADSC, and in six rabbits that received saline (control). Data are mean±SEM. #$P < 0.05$; control vs. the ADMPC-transplanted WHHL rabbit; &$P < 0.05$; the ADSC-transplanted WHHL rabbit vs. the ADMPC-transplanted WHHL rabbit). (**B**) Lipoprotein profiles in a representative WHHL rabbit with ADMP transplantation after gel filtration. Serum samples from the WHHL rabbit before and 4 weeks after transplantation were fractionated. Note the marked reduction in low-density lipoprotein (LDL) peak and appearance of a high-density lipoprotein (HDL) peak. (**C**) Rate of clearance of LDL from the serum of rabbits with and without transplantation of ADMPC. Animals were injected with ^{125}I-labeled human LDL, and the time course of clearance was monitored following trichloroacetic acid precipitation of serum at 5 min, 1 h, 2 h, 4 h, 6 h, and 28 h. Residual ^{125}I-LDL was expressed as a percentage of the signal at 5 min. The panel is the representative of two independent experiments. (**D**) DiO-LDL uptake into ADMPC-derived hepatocytes in the WHHL rabbit liver. Thin slices of recipient liver were incubated with DiO-labeled LDL in the serum-free medium for 24 h. After washing and fixation, the incubated slices were viewed by fluorescence microscopy. DiO-LDL-uptake cells (green) and no-uptake parenchymal cells are observed in the section. Bar = 100 μm.

3.5. In Situ Stem Cell Therapy by ADMPC

To determine the effects of ADMPC transplantation on the recipient rabbit lipid profile, serum cholesterol levels were monitored over 12 weeks (Fig. **4**, cited from reference 12 with modification). Significant reductions in total serum cholesterol were observed within 4 weeks of the transplantation, and the reductions were maintained for the entire period (Fig. **4A**). Furthermore, ADMPC-recipient animals showed significantly greater reductions than those in the control group. To determine the effects of ADMPC transplantation on the fractions of high-density lipoprotein and LDL in recipient animals, fractionation by fast protein liquid chromatography was performed (Fig. **4B**). Transplantation of ADMPC resulted in marked reduction of the peak LDL cholesterol and increment of high-density lipoprotein cholesterol fraction (right panel). Next, clearance experiments were performed with human LDL to confirm that the transplanted ADMPC contributed to the fall in serum cholesterol through uptake of LDL via LDL receptors. The rate of LDL clearance was significantly higher in the WHHL rabbits with transplanted ADMPC than WHHL rabbits without transplanted ADMPC (Fig. **4C**). Rabbits with ADMPC transplants showed ~2.4-fold (high-dose; 3 x 10^7 cells/rabbit) and

1.4-fold (low-dose; 5 x 10^6 cells/rabbit) increases in the rate of LDL cholesterol clearance over non-transplanted rabbits. To evaluate the uptake of DiO-LDL by transplants *ex vivo*, thin liver slices of WHHL rabbit were incubated with DiO-labeled LDL for 24 h and the uptake was examined as for the clearance experiments (Fig. **4D**). DiO-LDL was taken up by some but not all of the cells in the WHHL rabbit liver transplanted with ADMPC, with the positive cells observed dispersed, contacting, and integrating among the non DiO-LDL-positive parenchymal cells. This finding suggests that ADMPC differentiated into hepatocytes *in vivo*, thus lowering the serum cholesterol directly via LDL uptake.

3.6. ADMPC as a Promising Tool for Regenerative Medicine

For any successful regenerative medicine program, three issues must be considered: 1) what kind of tissues should be nominated as cell sources, 2) how should the cells be obtained from tissues, and 3) how will the cells behave after transplantation/administration. The following section discusses these considerations with respect to this study.

The source of stem cells for regenerative medicine should be easily and safely accessible as well as free of any ethical issues, thus allowing allogenic as well as autologous cellular therapy applications, and finally, the cell source should be available in large amounts. Adipose tissue is therefore a suitable cell source under these criteria. Liposuction surgery provides a safe method for collection of adipose tissue, harvesting from 100 ml to >3 L of lipoaspirate from material that is routinely discarded, thus avoiding any ethical concerns [16].

As to the second issue of cell processing, methods to isolate cells from adipose tissue were first reported in the 1960s [17-19]. Such methods involved mincing rat fat pads and incubating the resultant tissue fragments with collagenase. The digested material was then centrifuged to separate the floating population of mature adipocytes from the pelleted stromal vascular fraction (SVF). The SVF, which are sometimes referred to adipose tissue-derived regenerative cells (ADRC), consists of a heterogeneous cell population including fibroblasts, endothelial cells, pre-adipocytes, and mesenchymal stem cells [17-19]. However, as mentioned, this non-cultured cell population is too heterogeneous to apply therapeutically, necessitating the isolation of pre-adipocyte and/or mesenchymal stem cell-rich adherent cells from the SVF. The original procedure for this separation step was subsequently modified for the isolation of cells from human adipose tissue SVFs [20-23], and Zuk *et al.* [7] reported that the processed lipoaspirates exhibited mesenchymal stem cell-like features and could differentiate into adipocytes, osteocytes, and chondrocytes. Such cells are currently labeled as adipose tissue-derived stem cells (ADSC). The procedure used for obtaining these stem cells from lipoaspirates was described by Bjorntorp *et al.* [24] to obtain pre-adipocytes.

We have subsequently developed a novel isolation method for stem-like cells according to their adhesion properties [8-12]. As shown in Fig. (**1Aa**), fibroblast- and endothelial-like cells completely adhered onto the culture dish after 24 h in culture following the first-plating of the SVF. Most of the SVF cells were difficult to detach by conventional pipetting after this length of culture (24 h). However, a population of round self-aggregating cells that could only be detached by treatment with EDTA solution showed multilineage differentiation potency. In the EDTA-treating method, only cells of their properties with self-aggregation and EDTA-sensitiveness could be selected as ADMPC from plated SVF. In the conventional pre-plating methods to obtain ADSC [7, 24], the cells with EDTA-resistance could not be excluded. ADMPC exhibited high differentiation capacities for osteocytic, adipocytic, and chondrocytic lineages compared with ADSC, and could differentiate into hepatocyte-like cells, insulin-producing cells, and cardiomyoblast-like cells *in vitro* as non-mesenchymal lineages. We therefore named these cells ADMPC.

ADMPC differ from ADSC with regard to gene expression profiling. ADMPC express islet-1, a marker of undifferentiated cells and of cardiac, hepatic, and pancreatic progenitor cells [9-11]. Based on our findings, we propose that the islet-1-expressing ADMPC could be differentiated or reprogrammed into hepatocytes in the recipient liver *in vivo* after transplantation. In other words, the appropriate cells can show *in situ reprogramming* when transplanted and recruited into an appropriate environment.

Finally, we considered how the ADMPC would behave after transplantation/administration *in situ*. Traditionally, stem/progenitor cells are differentiated into terminally differentiated cells prior to transplantation/administration. For example, iPS cells are differentiated into neuronal cells and then applied for neuronal disease therapies. In these processes, researchers could mimic the relevant microenvironment and then differentiate the transplanted cells into the desired cell lineages. In contrast, we hypothesized that *in vitro* or *ex vivo* reprogramming could not sufficiently recapitulate the desired transplant microenvironment. Our concept is that the microenvironment *in situ* might supply cytokines to exert paracrine effects and form appropriate extracellular matrices, thus prompting the progenitor cells toward the desired terminal differentiation. ADMPC express islet-1, indicating that they might be appropriate progenitor cells on their own for *in situ* reprogramming as hepatocytes in the liver microenvironment. If these reprogrammed cells could correct given disease defects, clinical applications for *in situ* stem cell therapy become feasible.

In this review, we propose *in situ* stem cell therapy as a new tool for regenerative medicine and *in situ* reprogramming as a mechanism for the correction of disease. Yamanaka *et al.* [25] presented terminally differentiated cells that could be reprogrammed into the pluripotent state using only four factors. Followers confirmed the fact and named the concept "reprogramming". Melton *et al.* [26] subsequently showed that gene-modified cells alone could direct differentiation along a terminal path, and renamed the mechanism "direct reprogramming", and some cases of *ex vivo* gene therapy might be included in this concept. Here, we presented stem-like cells that could differentiate terminally *in situ* in the appropriate microenvironment.

4. CONCLUSIONS

In this review we describe ADMPC, novel adipose tissue-derived cells with stem cell-like properties and higher

differentiation potential than previously reported adipose tissue-derived cells. Not only could ADMPC differentiate into hepatocyte-like cells *in vitro*, but ADMPC *per se* also showed the same capacity in the hepatic environment and the *in situ* reprogrammed cells could correct the metabolic defect of diseased animals. The mechanisms described for *in situ* reprogramming hold great promise for applications in regenerative medicine as "*in situ* stem cell therapy".

ACKNOWLEDGMENTS

This study was supported in part by the Program for Promotion of Fundamental Studies in Health Sciences of the National Institute of Biomedical Innovation (NIBIO) and Kobe Translational Research Cluster, the Knowledge Cluster Initiative, Ministry of Education, Culture, Sports, Science and Technology (MEXT).

DISCLOSURE

It should be noted that the authors have previously published much of the material covered in this review article in "Tissue Eng Part C Methods", Volume 17, 2011, Pages 145-154.

CONFLICT OF INTEREST

The authors declare no conflict of interest.

REFERENCES

[1] Wagers AJ, Weissman IL. Plasticity of adult stem cells. *Cell* **2004**, 116, 639-648.

[2] Pittenger MF, Mackay AM, Beck SC, Jaiswal RK, Douglas R, Mosca JD Moorman MA, Simonetti DW, Craig S, Marshak DR. Multilineage potential of adult human mesenchymal stem cells. *Science* **1999**, 284, 143-147.

[3] Shih DT, Lee DC, Chen SC, Tsai RY, Huang CT, Tsai CC Shen EY, Chiu WT. Isolation and characterization of neurogenic mesenchymal stem cells in human scalp tissue. *Stem Cells* **2005**, 23, 1012-1020.

[4] In 't Anker PS, Scherjon SA, Kleijburg-van der Keur C, de Groot-Swings GM, Claas FH, Fibbe WE, Kanhai HH. Isolation of mesenchymal stem cells of fetal or maternal origin from human placenta. *Stem Cells* **2004**, 22, 1338-1345.

[5] Bieback K, Kern S, Klüter H, Eichler H. Critical parameters for the isolation of mesenchymal stem cells from umbilical cord blood. *Stem Cells* **2004**, 22, 625-634.

[6] Jiang Y, Jahagirdar BN, Reinhardt RL, Schwartz RE, Keene CD, Ortiz-Gonzalez XR, Reyes M, Lenvik T, Lund T, Blackstad M, Du J, Aldrich S, Lisberg A, Low WC, Largaespada DA, Verfaillie CM. Pluripotency of mesenchymal stem cells derived from adult marrow. *Nature* **2002**, 418, 41-49.

[7] Zuk PA, Zhu M, Ashjian P, De Ugarte DA, Huang JI, Mizuno H, Alfonso ZC, Fraser JK, Benhaim P, Hedrick MH. Human adipose tissue is a source of multipotent stem cells. *Mol Biol Cell* **2002**, 13, 4279-4295.

[8] Komoda H, Okura H, LeeC-M, Sougawa N, Iwayama T, Hashikawa T, Saga A, Yamamoto-Kakuta A, Ichinose A, Murakami S, Sawa Y, Matsuyama A. Reduction of Neu5GC Xenoantigen on Human ADMSCs lead to Them as Safer and More Useful Cell Sources for Realizing Various Stem Cell Therapies. *Tissue Eng Part A.* **2010**, 16, 1143-1155.

[9] Okura H, Matsuyama A, Lee CM, Saga A, Kakuta-Yamamoto A, Nagao A, Sougawa N, Sekiya N, Takekita K, Shudo Y, Miyagawa S, Komoda H, Okano T, Sawa Y. Cardiomyoblast-like cells differentiated from human adipose tissue-derived mesenchymal stem cells improve left ventricular dysfunction and survival in a rat myocardial infarction model. *Tissue Eng Part C Methods.* **2010**, 16, 417-425.

[10] Okura H, Komoda H, Saga A, Yamamoto-Kakuta A, Fumimoto Y, LeeC-M, Ichinose A, Sawa Y, Matsuyama A. Properties of hepatocyte-like cell clusters from human adipose tissue-derived mesenchymal stem cells. *Tissue Eng Part C Methods.* **2010**, 16, 761-770.

[11] Okura H, Fumimoto Y, Komoda H, Yanagisawa T, Nishida T, Noguchi S Sawa Y., Matsuyama A. Transdifferentiation of Human Adipose Tissue-Derived Stromal Cells into Insulin-Producing Clusters. *J Artif Organs.* **2009**, 12, 123-130.

[12] Okura H, Saga A, Fumimoto Y, Soeda M, Moriyama M, Moriyama H, Nagai K, Lee CM, Yamashita S, Ichinose A, Hayakawa T, Matsuyama A. Transplantation of human adipose tissue-derived multilineage progenitor cells reduces serum cholesterol in hyperlipidemic Watanabe rabbits. *Tissue Eng Part C Methods.* **2011**, 17, 145-154.

[13] Saga A, Okura H, Soeda M, Tani J, Fumimoto Y, Komoda H, Moriyama M, Moriyama H, Yamashita S, Ichinose A, Daimon T, Hayakawa T, Matsuyama A. HMG-CoA reductase inhibitor augments the serum total cholesterol-lowering effect of human adipose tissue-derived multilineage progenitor cells in hyperlipidemic homozygous Watanabe rabbits. *Biochem Biophys Res Commun.* **2011**, 412, 50-54.

[14] Hosono T, Mizuguchi H, Katayama K, Koizumi N, Kawabata K, Yamaguchi T, Nakagawa S, Watanabe Y, Mayumi T, Hayakawa T. RNA interference of PPARgamma using fiber-modified adenovirus vector efficiently suppresses preadipocyte-to-adipocyte differentiation in 3T3-L1 cells. *Gene* **2005**, 348, 157-165.

[15] Yanagita M, Kashiwagi Y, Kobayashi R, Tomoeda M, Shimabukuro Y, Murakami S. Nicotine inhibits mineralization of human dental pulp cells. *J Endod.* **2008**, 34, 1061-1065.

[16] Katz AJ, Llull R, Hedrick MH, Futrell JW. Emerging approaches to the tissue engineering of fat. *Clin Plast Surg* **1999**, 26, 587–603

[17] Rodbell M. Metabolism of isolated fat cells. II. The similar effects of phospholipase c (*Clostridium perfringens* alpha toxin) and of insulin on glucose and amino acid metabolism. *J Biol Chem.* **1966**, 241, 130–139.

[18] Rodbell M. The metabolism of isolated fat cells. IV. Regulation of release of protein by lipolytic hormones and insulin. *J Biol Chem.* **1966**, 241, 3909–3917.

[19] Rodbell M, Jones AB. Metabolism of isolated fat cells. III. The similar inhibitory action of phospholipase c (clostridium perfringens alpha toxin) and of insulin on lipolysis stimulated by lipolytic hormones and theophylline. *J Biol Chem.* **1966**, 241, 140–142.

[20] Van RL, Bayliss CE, Roncari DA. Cytological and enzymological characterization of adult human adipocyte precursors in culture. *J Clin Invest.* **1976**, 58, 699–704.

[21] Björntorp P, Karlsson M, Gustafsson L, Smith U, Sjöström L, Cigolini M, Storck G, Pettersson P. Quantitation of different cells in the epididymal fat pad of the rat. *J Lipid Res.* **1979**, 20, 97-106

[22] Deslex S, Negrel R, Vannier C, Etienne J, Ailhaud G. Differentiation of human adipocyte precursors in a chemically defined serum-free medium. *Int J Obes.* **1987**, 11, 19–27.

[23] Hauner H, Entenmann G, Wabitsch M, Gaillard D, Ailhaud G, Negrel R, Pfeiffer EF. Promoting effect of glucocorticoids on the differentiation of human adipocyte precursor cells cultured in a chemically defined medium. *J Clin Invest.* **1989**, 84, 1663–1670.

[24] Bjorntorp P, Karlsson M, Pertoft H, Pettersson P, Sjostrom L, Smith U. Isolation and characterization of cells from rat adipose tissue developing into adipocytes. *J Lipid Res.* **1978**, 19, 316–324.

[25] Yamanaka S. Strategies and new developments in the generation of patient-specific pluripotent stem cells. *Cell Stem Cell.* **2007**, 1, 39-49.

[26] Gurdon JB, Melton DA. Nuclear reprogramming in cells. *Science* **2008**, 322, 1811-1815.

Received: October 24, 2011 Revised: December 02, 2011 Accepted: January 03, 2012

Age-Dependent Decline of Association Between Obesity and Hyperglycemia in Men and Women

ICHIRO WAKABAYASHI, PHD, MD[1]
TAKASHI DAIMON, PHD[2]

OBJECTIVE—The purpose of this study was to determine whether age influences the association between obesity and hyperglycemia.

RESEARCH DESIGN AND METHODS—The subjects were 57,576 Japanese male and female workers aged 35–70 years. The associations of adiposity indices, including BMI, waist circumference, and waist-to-height ratio, with risk for hyperglycemia were compared among different age groups (35–39, 40–49, 50–59, and 60–70 years) using odds ratios (ORs).

RESULTS—There were significant trends for the crude ORs of obese subjects versus nonobese subjects for hyperglycemia to be lower as age increased in men and women. Multivariate logistic regression analysis showed these trends of age-dependent decreases in ORs for hyperglycemia were not altered by adjustment for confounders such as smoking, alcohol drinking, and habitual exercise.

CONCLUSIONS—The results suggest that the association between obesity and hyperglycemia declines with age in men and women.

Diabetes Care 35:175–177, 2012

A J- or U-shaped relationship is known to exist between BMI and all-cause mortality (1,2). Excess mortality in obese people is mainly due to vascular disease (3) and has been shown to decline with age (4–7). Type 2 diabetes is a major risk factor for cardiovascular disease and is induced by lifestyle-related modifiable risk factors such as obesity and low physical activity. The association between obesity and the risk for coronary heart disease has been shown to be weaker in older men than in younger men (8,9). The incidence of type 2 diabetes increases with age (10); however, the effects of age on the relationship between obesity and glycemic status have not been confirmed. Therefore, the aim of this study was to clarify whether the association between obesity and hyperglycemia differs by age in men and women.

RESEARCH DESIGN AND METHODS

Subjects

The subjects were Japanese workers (37,686 men and 19,890 women), aged 35–70 years, who had received periodic health examinations at workplaces in Yamagata Prefecture in Japan and were divided into four groups by age (35–39, 40–49, 50–59, and 60–70 years). Histories of alcohol consumption, cigarette smoking, habitual exercise, and treatment for any illnesses were surveyed by questionnaires. This study was approved by the Yamagata University School of Medicine Ethics Committee.

Measurements

BMI was calculated as weight in kilograms divided by the square of height in meters. The criterion for obesity evaluated by using each adiposity index was defined as BMI $\geq$25 kg/m^2, waist circumference $\geq$85 cm for men and $\geq$80 cm for women, and waist-to-height ratio (WHtR) $\geq$0.5. Fasted blood was sampled from each subject, and hemoglobin A_{1c}, triglycerides, and LDL cholesterol were determined. The hemoglobin A_{1c} values were calibrated by using a formula proposed by the Japan Diabetes Society (11) as hemoglobin A_{1c} (National Glycohemoglobin Standardization Program) (%) = hemoglobin A_{1c} (Japan Diabetes Society) (%) + 0.4%. Hyperglycemia including diabetes and prediabetes was defined as hemoglobin A_{1c} $\geq$5.7% (12) and/or current history of drug therapy for diabetes.

Statistical analysis

Statistical analyses were performed using SPSS 16.0 J software (SPSS Inc., Chicago, IL). Crude odds ratios (ORs) and ORs after adjustment for age, smoking, alcohol intake, and habitual exercise were calculated by using logistic regression. Trends for crude ORs across the age groups were tested by using the Breslow-Day test. P values < 0.05 were defined as significant.

RESULTS—Prevalences of hyperglycemia, high triglycerides, and high LDL cholesterol were, respectively, 24.2, 36.0, and 21.3% in men and 19.3, 14.1, and 19.4% in women. Prevalences of high BMI, large waist circumference, and high WHtR were, respectively, 30.8, 44.2, and 46.5% in men and 20.6, 41.3, and 47.8% in women.

In all of the age groups of men and women, crude and adjusted ORs for hyperglycemia of subjects with a high or large adiposity index versus subjects without a high or large adiposity index were significantly higher compared with a reference level of 1.00 (Table 1). There were significant trends for the crude ORs for hyperglycemia to be lower in higher age groups, and the adjusted ORs also tended to be lower as age increased. Crude and adjusted ORs for high triglycerides and high LDL cholesterol of subjects with a high or large adiposity index versus subjects without a high or large adiposity index also tended to decrease with age in men and women (Table 1).

From the [1]Department of Environmental and Preventive Medicine, Hyogo College of Medicine, Nishinomiya, Hyogo, Japan; and the [2]Division of Biostatistics, Hyogo College of Medicine, Nishinomiya, Hyogo, Japan.
Corresponding author: Ichiro Wakabayashi, wakabaya@hyo-med.ac.jp.
Received 12 September 2011 and accepted 18 October 2011.
DOI: 10.2337/dc11-1775

Table 1—*ORs for hyperglycemia, high triglycerides, and high LDL cholesterol of subjects with a high or large adiposity index versus subjects without a high or large adiposity index in men and women*

	Hyperglycemia			High triglycerides			High LDL cholesterol		
Variable	High BMI	Large WC	High WHtR	High BMI	Large WC	High WHtR	High BMI	Large WC	High WHtR
Men									
35–39 years									
Crude	4.45 (3.73–5.32)*	4.06 (3.38–4.88)*	4.47 (3.73–5.35)*	3.69 (3.28–4.15)*	3.40 (3.03–3.81)*	3.70 (3.30–4.16)*	3.03 (2.66–3.45)*	3.18 (2.79–3.62)*	2.98 (2.62–3.40)*
Adjusted	4.16 (3.47–4.97)*	3.92 (3.26–4.71)*	4.25 (3.55–5.11)*	3.74 (3.32–4.22)*	3.39 (3.02–3.80)*	3.71 (3.29–4.17)*	2.90 (2.54–3.31)*	3.10 (2.72–3.53)*	2.88 (2.53–3.29)*
40–49 years									
Crude	3.41 (3.10–3.76)*	2.96 (2.68–3.27)*	3.13 (2.84–3.45)*	2.83 (2.62–3.06)*	3.05 (2.82–3.28)*	2.92 (2.71–3.15)*	2.17 (1.99–2.36)*	2.26 (2.08–2.46)*	2.34 (2.15–2.55)*
Adjusted	3.39 (3.08–3.73)*	2.95 (2.67–3.26)*	3.07 (2.78–3.38)*	2.87 (2.65–3.10)*	3.02 (2.80–3.26)*	2.91 (2.70–3.14)*	2.11 (1.94–2.30)*	2.26 (2.07–2.46)*	2.32 (2.13–2.52)*
50–59 years									
Crude	2.50 (2.31–2.70)*	2.21 (2.05–2.38)*	2.25 (2.09–2.42)*	2.35 (2.18–2.53)*	2.75 (2.56–2.95)*	2.74 (2.55–2.95)*	1.81 (1.66–1.97)*	1.87 (1.72–2.03)*	1.81 (1.66–1.97)*
Adjusted	2.49 (2.31–2.69)*	2.24 (2.08–2.41)*	2.23 (2.07–2.40)*	2.37 (2.19–2.55)*	2.74 (2.55–2.95)*	2.80 (2.60–3.01)*	1.77 (1.62–1.93)*	1.87 (1.72–2.04)*	1.82 (1.68–1.99)*
60–70 years									
Crude	1.80 (1.60–2.02)*	1.75 (1.57–1.95)*	1.73 (1.54–1.93)*	2.23 (1.98–2.51)*	2.64 (2.35–2.96)*	2.96 (2.61–3.36)*	1.38 (1.19–1.60)*	1.51 (1.32–1.74)*	1.72 (1.48–2.00)*
Adjusted	1.78 (1.59–2.00)*	1.76 (1.58–1.97)*	1.72 (1.54–1.93)*	2.22 (1.96–2.50)*	2.63 (2.34–2.96)*	3.06 (2.70–3.48)*	1.37 (1.17–1.59)*	1.58 (1.37–1.82)*	1.80 (1.54–2.10)*
Trend (*P*)	< 0.001	< 0.001	< 0.001	< 0.001	< 0.001	< 0.001	< 0.001	< 0.001	< 0.001
Women									
35–39 years									
Crude	5.91 (4.24–8.24)*	4.66 (3.34–6.51)*	4.79 (3.42–6.71)*	5.87 (4.30–8.00)*	4.82 (3.53–6.57)*	5.17 (3.77–7.08)*	5.47 (4.11–7.29)*	4.50 (3.40–5.97)*	4.94 (3.72–6.57)*
Adjusted	5.83 (4.17–8.14)*	4.68 (3.34–6.54)*	4.76 (3.39–6.67)*	5.93 (4.34–8.11)*	4.81 (3.52–6.57)*	5.17 (3.78–7.09)*	5.42 (4.05–7.24)*	4.54 (3.42–6.03)*	4.96 (3.72–6.61)*
40–49 years									
Crude	4.04 (3.49–4.68)*	3.42 (2.96–3.95)*	3.47 (3.00–4.02)*	4.32 (3.70–5.03)*	4.09 (3.50–4.77)*	3.84 (3.28–4.49)*	3.27 (2.84–3.75)*	2.76 (2.42–3.14)*	2.75 (2.41–3.14)*
Adjusted	4.01 (3.46–4.65)*	3.37 (2.92–3.89)*	3.35 (2.89–3.88)*	4.15 (3.55–4.85)*	3.99 (3.41–4.66)*	3.71 (3.16–4.35)*	3.16 (2.75–3.64)*	2.69 (2.36–3.07)*	2.64 (2.31–3.02)*
50–59 years									
Crude	2.56 (2.29–2.87)*	2.23 (2.01–2.47)*	2.29 (2.05–2.55)*	2.55 (2.25–2.89)*	2.60 (2.31–2.94)*	3.02 (2.64–3.45)*	1.72 (1.54–1.93)*	2.02 (1.82–2.24)*	2.20 (1.97–2.45)*
Adjusted	2.56 (2.28–2.86)*	2.18 (1.96–2.41)*	2.19 (1.97–2.45)*	2.50 (2.20–2.83)*	2.56 (2.26–2.89)*	2.98 (2.60–3.41)*	1.79 (1.59–2.01)*	2.05 (1.85–2.28)*	2.22 (1.99–2.48)*
60–70 years									
Crude	2.16 (1.74–2.69)*	1.68 (1.38–2.04)*	1.50 (1.21–1.86)*	1.96 (1.54–2.49)*	2.26 (1.78–2.87)*	2.16 (1.64–2.84)*	1.25 (0.99–1.58)	1.45 (1.18–1.79)*	1.48 (1.17–1.87)*
Adjusted	2.10 (1.68–2.62)*	1.65 (1.36–2.02)*	1.46 (1.17–1.82)*	1.91 (1.49–2.43)*	2.25 (1.76–2.87)*	2.16 (1.63–2.87)*	1.29 (1.02–1.64)†	1.52 (1.23–1.89)*	1.57 (1.24–2.00)*
Trend (*P*)	<0.001	<0.001	<0.001	<0.001	<0.001	<0.001	<0.001	<0.001	<0.001

Crude and adjusted ORs (95% CI) for hyperglycemia, high triglycerides, and high LDL cholesterol are shown. Adjusted ORs were calculated using age, smoking, alcohol drinking, and habitual exercise as other explanatory variables in logistic regression analysis. Therapy for dyslipidemia was also added to explanatory variables for calculation of ORs for high triglycerides and high LDL cholesterol. *P* values for trends across the age groups are also shown. WC, waist circumference. *$P < 0.001$. †$P < 0.05$.

CONCLUSIONS—The association between obesity and hyperglycemia declined with age in men and women, although the association remained significant even in the highest age group. This age-dependent trend was consistent in any analyses using different adiposity-related indices. This study is, to the best of our knowledge, the first study showing an age-dependent significant attenuation of the association between obesity and glycemic status both in men and women. In addition, significant age-dependent declines were also found in the associations of obesity with dyslipidemias such as high triglycerides and high LDL cholesterol. Therefore, the associations between obesity and metabolic disorders, such as diabetes and dyslipidemia, are thought to decline with age.

There is limited information on whether and how age influences the relationship between obesity and diabetes. Two recent studies have reported results related to this topic. Effects of obesity evaluated by BMI on incidence of type 2 diabetes have been reported to decline with age in women but not in men, and the authors speculated that the sex difference observed was due to the smaller population size of male subjects than that of female subjects (13). Another study showed that the correlation coefficient between waist circumference and fasting blood glucose tended to be higher in younger (≤51 years) than in older (>51 years) men and women, although the differences in the correlation between the younger and older subjects were not significant (14). The current study clearly demonstrated significant age-dependent declines of the associations of obesity with hyperglycemia and dyslipidemia in men and women.

Taken together with these findings, our results suggest that the effect of obesity on development of diabetes is stronger in younger people than in older people. This also suggests that correction of obesity is more effective for prevention of diabetes in younger people than in older people and agrees with a consensus that young people should be encouraged to attain and maintain a weight-for-height ratio in the normal range to prevent type 2 diabetes (15). The age-dependent declines in the associations of obesity with hyperglycemia and dyslipidemia may partly explain the weaker association between obesity and the risk for coronary heart disease in older men than in younger men (8,9).

In conclusion, the association between obesity and hyperglycemia is stronger in younger men and women than in older men and women, respectively, and this finding supports a general concept of the necessity of body weight control in young people from the viewpoint of prevention of type 2 diabetes.

Acknowledgments—This work was supported by a Grant-in-Aid for Scientific Research from the Japan Society for the Promotion of Science (21390211).

No potential conflicts of interest relevant to this article were reported.

I.W. researched data, performed the statistical analyses, wrote the manuscript, and is guarantor for the article. T.D. performed the statistical analyses.

References

1. Klenk J, Nagel G, Ulmer H, et al.; The VHM&PP Study Group. Body mass index and mortality: results of a cohort of 184,697 adults in Austria. Eur J Epidemiol 2009;24:83–91
2. Berrington de Gonzalez A, Hartge P, Cerhan JR, et al. Body-mass index and mortality among 1.46 million white adults. N Engl J Med 2010;363:2211–2219
3. Whitlock G, Lewington S, Sherliker P, et al.; Prospective Studies Collaboration. Body-mass index and cause-specific mortality in 900 000 adults: collaborative analyses of 57 prospective studies. Lancet 2009;373:1083–1096
4. Bender R, Jöckel KH, Trautner C, Spraul M, Berger M. Effect of age on excess mortality in obesity. JAMA 1999;281:1498–1504
5. Stevens J, Cai J, Juhaeri, Thun MJ, Williamson DF, Wood JL. Consequences of the use of different measures of effect to determine the impact of age on the association between obesity and mortality. Am J Epidemiol 1999;150:399–407
6. Reuser M, Bonneux L, Willekens F. The burden of mortality of obesity at middle and old age is small. A life table analysis of the US Health and Retirement Survey. Eur J Epidemiol 2008;23:601–607
7. Kuk JL, Ardern CI. Influence of age on the association between various measures of obesity and all-cause mortality. J Am Geriatr Soc 2009;57:2077–2084
8. Rimm EB, Stampfer MJ, Giovannucci E, et al. Body size and fat distribution as predictors of coronary heart disease among middle-aged and older US men. Am J Epidemiol 1995;141:1117–1127
9. Shiraishi J, Kohno Y, Sawada T, et al.; The AMI-Kyoto Multi-Center Risk Study Group. Relation of obesity to acute myocardial infarction in Japanese patients. Differences in gender and age. Circ J 2006;70:1525–1530
10. Jack L Jr, Boseman L, Vinicor F. Aging Americans and diabetes. A public health and clinical response. Geriatrics 2004;59:14–17
11. The Committee of Japan Diabetes Society on the diagnostic criteria of diabetes mellitus. Report of the committee on the classification and diagnostic criteria of diabetes mellitus. J Japan Diab Soc 2010;53:450–467 [in Japanese]
12. American Diabetes Association. Diagnosis and classification of diabetes mellitus. Diabetes Care 2011;34(Suppl. 1):S62–S69
13. Fujita M, Ueno K, Hata A. Effect of obesity on incidence of type 2 diabetes declines with age among Japanese women. Exp Biol Med (Maywood) 2009;234:750–757
14. Oda E, Kawai R. Age- and gender-related differences in correlations between abdominal obesity and obesity-related metabolic risk factors in Japanese. Intern Med 2009;48:497–502
15. Bloomgarden ZT. Prevention of obesity and diabetes. Diabetes Care 2003;26:3172–3178

Biochemical and Biophysical Research Communications 412 (2011) 50–54

Contents lists available at ScienceDirect

Biochemical and Biophysical Research Communications

journal homepage: www.elsevier.com/locate/ybbrc

HMG-CoA reductase inhibitor augments the serum total cholesterol-lowering effect of human adipose tissue-derived multilineage progenitor cells in hyperlipidemic homozygous Watanabe rabbits

Ayami Saga [a], Hanayuki Okura [a], Mayumi Soeda [a], Junko Tani [a], Yuichi Fumimoto [a], Hiroshi Komoda [a], Mariko Moriyama [a,b], Hiroyuki Moriyama [b], Shizuya Yamashita [c], Akihiro Ichinose [d], Takashi Daimon [e], Takao Hayakawa [b], Akifumi Matsuyama [a,*]

[a] Department of Somatic Stem Cell Therapy and Health Policy, Foundation for Biomedical Research and Innovation, TRI305, 1-5-4 Minatojima-minamimachi, Chuo-ku, Kobe, Hyogo 650-0047, Japan
[b] Pharmaceutical Research and Technology Institute, Kinki University, 3-4-1 Kowakae, Higashi-Osaka, Osaka 577-8502, Japan
[c] Division of Cardiology, Department of Internal Medicine, Osaka University Graduate School of Medicine, Suita, Osaka 565-0871, Japan
[d] Department of Plastic Surgery, Kobe University Hospital, 7-5-2 Kusunoki-cho, Chuo-ku, Kobe, Hyogo 660-0017, Japan
[e] Division of Biostatistics, Hyogo College of Medicine, 1-1 Mukogawa-cho, Nishinomiya, Hyogo 663-8501, Japan

ARTICLE INFO

Article history:
Received 7 July 2011
Available online 22 July 2011

Keywords:
ADMPC
WHHL
HMG-CoA reductase inhibitor
Pravastatin
Cholesterol
Cell therapy

ABSTRACT

Familial hypercholesterolemia (FH) is an autosomal codominant disease characterized by high concentrations of proatherogenic lipoproteins secondary to deficiency in low-density lipoprotein (LDL) receptor. We reported recently the use of *in situ* stem cell therapy of human adipose tissue-derived multilineage progenitor cells (hADMPCs) in lowering serum total cholesterol in the homozygous Watanabe heritable hyperlipidemic (WHHL) rabbits, an animal model of homozygous FH. Here we demonstrate that pravastatin, an HMG-CoA reductase inhibitor, augmented the cholesterol-lowering effect of transplanted hADMPCs and enhanced LDL clearance in homozygous WHHL rabbit. The results suggest the potential beneficial effects of *in situ* stem cell therapy in concert with appropriately selected pharmaceutical agents, in regenerative medicine.

1. Introduction

Familial hypercholesterolemia (FH) is characterized by premature and accelerated development of atherosclerotic lesions caused by elevated levels of cholesterol-rich lipoproteins in plasma. The disease is caused by mutations in the low-density lipoprotein (LDL) receptor gene that result in a significant decrease in receptor-mediated uptake of lipoproteins from the circulation [1–3]. Patients homozygous for defects in LDL receptors have serum cholesterol levels 5–10 times those of normal and suffer as early as the first two decades of life serious complications such as coronary artery disease [4,5]. In homozygous FH patients, conventional drug therapy such as HMG-CoA reductase inhibitors, collectively known as "statins", cannot treat the condition, and therapeutic recourses are limited to chronic plasmapheresis and orthotopic liver transplantation [1]. Although liver transplants lower LDL levels, the procedure is life threatening and, in addition, donor livers are in short supply. A number of gene therapy approaches have shown some promise in animal models and human [6–9]. As an alternative to whole-organ transplantation and/or gene therapy, cellular transplantation has been proposed to provide functional LDL receptors for the treatment of hypercholesterolemia. Transplantation of allogenic and xenogenic hepatocytes is reported to be effective in lowering serum cholesterol in the Watanabe heritable hyperlipidemic (WHHL) rabbit [10–13], which is an animal model of homozygous FH. In this context, we have reported the ability of human adipose tissue-derived multilineage progenitor cells (hADMPCs) to differentiate into hepatocytes both *in vitro* and *in vivo* and to rectify critical liver functions [14,15] similar to reports from other laboratories [16,17]. Various groups have demonstrated the *in vitro* differentiation of hADMPCs into various cell types and confirmed that hADMPCs can be easily and safely obtained in large quantities without serious ethical issues [14,15,18,19]. In homozygous FH patients, HMG-CoA reductase inhibitors have no effect on the condition as mentioned [20]. We hypothesized that HMG-CoA reductase inhibitor can act in concert with *in situ* differentiated hepatocyte-like cells originating from transplanted hADMPCs to lower serum cholesterol

* Corresponding author. Fax: +81 78 304 8707.
E-mail address: akifumi-matsuyama@umin.ac.jp (A. Matsuyama).

0006-291X/$ - see front matter © 2011 Elsevier Inc. All rights reserved.
doi:10.1016/j.bbrc.2011.07.035

levels in hyperlipidemia. To test our hypothesis, we tested the effects of treatment with HMG-CoA reductase inhibitor in hADMPC-transplanted homozygous WHHL rabbits.

2. Materials and methods

2.1. Adipose tissue samples

Subcutaneous adipose tissue samples (10–50 g, each) were resected during plastic surgery in 5 females (age, 20–60 years) as excess discards. The study protocol was approved by the Review Board for Human Research of Kobe University Graduate School of Medicine, Osaka University Graduate School of Medicine, Kinki University Pharmaceutical Research and Technology Institute and Foundation for Biomedical Research and Innovation. Each subject provided a signed informed consent.

2.2. isolation of hADMPCs

The hADMPCs were prepared as described previously [21] with some modification [14,15,18,19]. Briefly, the resected excess adipose tissue was minced and then digested at 37 °C for 1 h in Hank's balanced salt solution (HBSS, GIBCO Invitrogen, Grand Island, NY) containing 0.075% collagenase type I (Sigma Aldrich, St. Louis, MO). Digests were filtered through a cell strainer (BD Bioscience, San Jose, CA) and centrifuged at 800 *g* for 10 min. Erythrocytes were excluded using density gradient centrifugation with Lymphoprep ($d = 1.077$; Nycomed, Oslo, Norway), and the remaining cells were cultured in Dulbecco's modified Eagle's medium (DMEM, GIBCO Invitrogen) with 10% defined fetal bovine serum (FBS, GIBCO Invitrogen) for 24 h at 37 °C. Following incubation, the adherent cells were washed extensively and then treated with 0.2 g/l ethylenediaminetetraacetate (EDTA) solution (Nacalai Tesque, Kyoto, Japan). The resulting suspended cells were replated at a density of 10,000 cells/cm^2 on human fibronectin (FN)-coated dishes (AGC, Tokyo, Japan) in Stem Cell Medium (Nipro, Osaka, Japan), 1× insulin-transferring selenium (ITS, GIBCO Invitrogen), 1 nM dexamethasone (Sigma–Aldrich), 100 μM ascorbic acid 2-phosphate (Sigma Aldrich), 10 ng/ml epidermal growth factor (EGF, PeproTec, Rocky Hill, NJ), and 5% FBS (GIBCO Invitrogen). After 5–6 passages, the hADMPCs were used for transplantation.

2.3. hADMPCs transplantation and immunosuppression/statin treatment regimen

The transplantation procedure was performed as reported previously [15]. Briefly, 8-week-old homozygous WHHL rabbits (Kitayamalabes, Inc., Japan) ($n = 7$) were anesthetized with pentobarbital (50 mg/kg) and an incision distal and parallel to the lower end of the ribcage was made. The peritoneum was incised and hADMPCs (3×10^7 cells) suspended in 3 mL of HBSS (20 °C) with heparin were infused within 5 min into the portal vein via a 18-gauge Angiocath™ (BD, UT) (Fig. 1A). The immunosuppression regimen (Fig. 1B) consisted of the following: (i) intramuscular injection of cyclosporin A (6 mg/kg/day) daily from the day before surgery to sacrifice; (ii) intramuscular injection of rapamycin (0.05 mg/kg/day) daily from the day before surgery to sacrifice; (iii) methylprednisolone at 3 mg/kg/day (day −1 to 7), followed by tapering to 2 mg/kg/day (day 8–14), 1 mg/kg/day (day 15–21) and 0.5 mg/kg/day (day 22 to sacrifice); (iv) intravenous injection of cyclophosphamide (20 mg/kg/day) at day 0, 2, 5 and 7; (v) intramuscular injection of ganciclovir (2.5 mg/kg/day) was also administrated to avoid viral infection in the immunocompromised host. Twelve weeks after hADMPCs transplantation, the rabbits were divided into two groups; the first was treated with low dose pravastatin (0.75 mg/kg/day i.m., $n = 4$), an HMG-CoA reductase inhibitor (treatment group), while the second served as the control and injected intramuscularly with the vehicle ($n = 3$).

2.4. Assay for lipid profiling

Serum samples were obtained from nonfasting rabbits before and after pravastatin treatment (at 12 and 16 weeks). Serum total cholesterol and HDL-cholesterol fraction were measured using assay kits from Wako Pure Chemical Industries (Osaka, Japan)

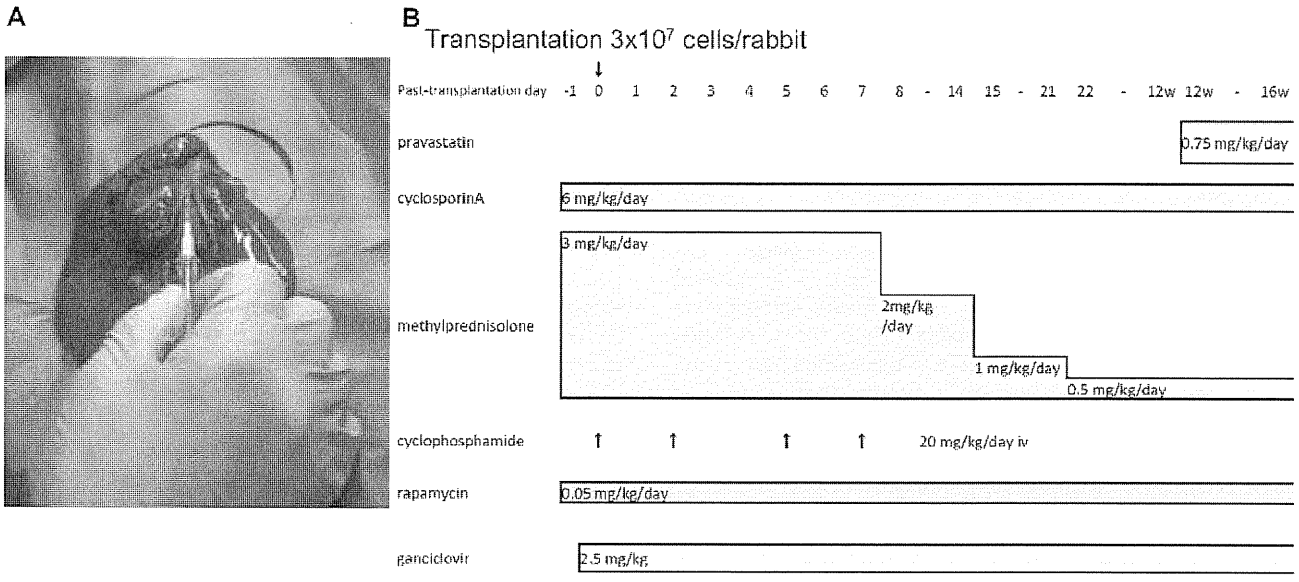

Fig. 1. (A) Surgical procedure. Watanabe heritable hyperlipidemic (WHHL) rabbits were anesthetized with pentobarbital. An incision was made distal and parallel to the lower end of the ribcage. The peritoneum was incised and hADMPCs (3×10^7 cells/rabbit) were infused into the portal vein using an 18-gauge Angiocath. (B) Immunosuppression regimen. Cyclosporin A (6 mg/kg/day) and rapamycin (0.05 mg/kg/day) were administered intramuscularly daily from the day before surgery to sacrifice. Methylprednisolone was administered at 3 mg/kg/day (days 1–7), 2 mg/kg/day (days 8–14), 1 mg/kg/day (days 15–21), and 0.5 mg/kg/day (day 22 to sacrifice). Cyclophosphamide (20 mg/kg/day) was injected intravenously at days 0, 2, 5, and 7. Ganciclovir (2.5 mg/kg/day) was also injected intramuscularly to avoid viral infection in the immunocompromised host. Twelve weeks after hADMPCs transplantation, hADMPC-transplanted WHHL rabbit were divided into two groups; the pravastatin-treated group ($n = 4$) and the control vehicle group ($n = 3$).

and the before and after treatment with/without pravastatin were compared in the two groups.

2.5. Clearance of ^{125}I-LDL from rabbit serum

LDL turnover study was performed as reported previously to examine the clearance of ^{125}I-LDL from rabbit serum [15]. Briefly, at the end of the study (Fig. 1B), the animals were examined for the LDL turnover assay. ^{125}I-human LDL (BT-913R, Biomedical Technologies Inc., Stoughton, MA) was delivered via the marginal ear vein of the WHHL rabbits and normal control rabbits in physiological saline containing 2 mg/mL bovine serum albumin. Blood was collected from the opposite ear after injection at 5 min, 1, 2, 3, 4, 6, 24 and 28 h. ^{125}I-labeled apolipoprotein B-containing LDL was precipitated with 20% of trichloroacetic acid (Wako Pure Chemical Industries) (serum; 320 μL, 100% w/v TCA 80 μL), and then the precipitants were applied for counting.

2.6. Statistical analysis

Values were expressed as mean ± SEM. Differences between mean values before and after treatment in the treated and untreated groups were evaluated using the paired *t*-test or Student's *t*-test. A *P* value less than 0.05 was considered statistically significant. All statistical analyses were performed using the SPSS Statistics 17.0 package (SPSS Inc., Chicago, IL).

3. Results

Pravastatin treatment significantly reduced serum total cholesterol level in hADMPC-transplanted homozygous WHHL rabbits ($n = 4$, before: 410 ± 35, after: 291 ± 46 mg/dL, $p = 0.0382$, Fig. 2), whereas control hADMPC-transplanted WHHL rabbits showed no such fall ($n = 3$, before: 409 ± 63, after: 375 ± 53 mg/dL, Fig. 2). On the other hand, the fall in HDL-cholesterol was not significant in both the pravastatin and control vehicle rabbits (pravastatin group: before 24.3 ± 0.5, after 23.3 ± 0.3 mg/dL, control vehicle group: before 22.8 ± 2.2, after 20.8 ± 2.2 mg/dL, Fig. 2).

Next, we measured human LDL clearance in order to confirm that the fall in serum total cholesterol induced by pravastatin in the hADMPCs-transplanted rabbits was mediated through human LDL receptors on hADMPC-derived hepatocytes (Fig. 3). Pravastatin shifted the LDL-turnover curve to the left ($n = 4$) (Fig. 3A). Furthermore, pravastatin significantly increased the 24-h LDL-clearance rate in the hADMPC-transplanted WHHL rabbits ($n = 4$, 95.0 ± 0.6%) compared to the control ($n = 3$, 90.7 ± 0.2%, $p = 0.0429$, Fig. 3).

4. Discussion

The main finding of this study was that pravastatin enhanced the lipid-lowering effects and the LDL-clearance rate of transplanted hADMPCs in spontaneously hyperlipidemic homozygous WHHL rabbits.

An important issue in cellular therapy is the cell source selected for clinical application. The major advantages of hADMPCs are their availability through simple harvesting surgical procedure and lack of ethical obstacles. In fact, a simple liposuction surgery yields massive amount of lipoaspirate adipose tissue, ranging from 100 ml to >3 L [22]. Our previous study in homozygous WHHL rabbits showed that human LDL binds to the receptors on hADMPC-derived hepatocytes and such human LDL receptors compensate the non-functional mutant LDL receptors in the WHHL rabbit [15]. Moreover, hepatocytes derived from hADMPCs have the advantage of expressing LDL receptor from an endogenous gene with intact regulatory sequences. These findings prompted us to test the effect of HMG-CoA reductase inhibitor on serum total cholesterol in hyperlipidemic rabbits transplanted with hADMPCs.

Among the numerous enzymes involved in the cholesterol biosynthesis pathway, HMG-CoA reductase plays an essential in cholesterol synthesis. Inhibition of the HMG-CoA enzyme by pravastatin decreases LDL-cholesterol by the following mechanisms: *de novo* decrease in cholesterol synthesis, simultaneous increase in

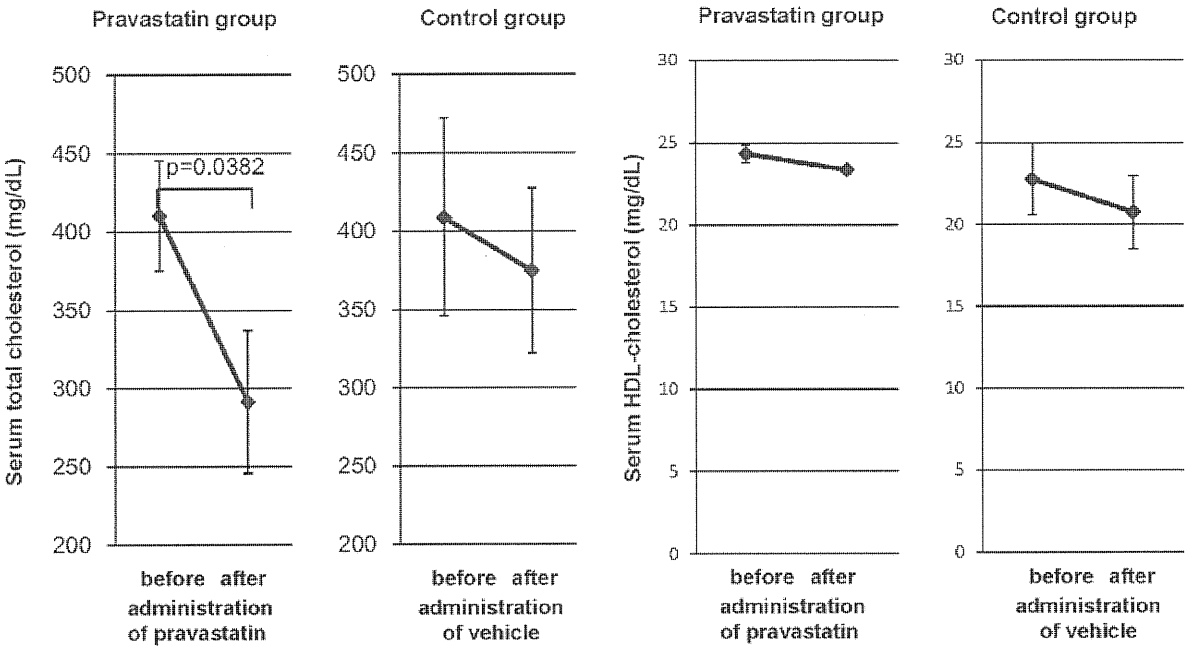

Fig. 2. Serum total cholesterol (*left*) and serum HDL-cholesterol (*right*) in hADMPC-transplanted homozygous WHHL rabbits before and after administration of pravastatin ($n = 4$) or the vehicle ($n = 3$). Data are mean ± SEM. Differences between mean values before and after administration of in the pravastatin or the vehicle were evaluated using the paired *t*-test. A *P* value less than 0.05 was considered statistically significant.

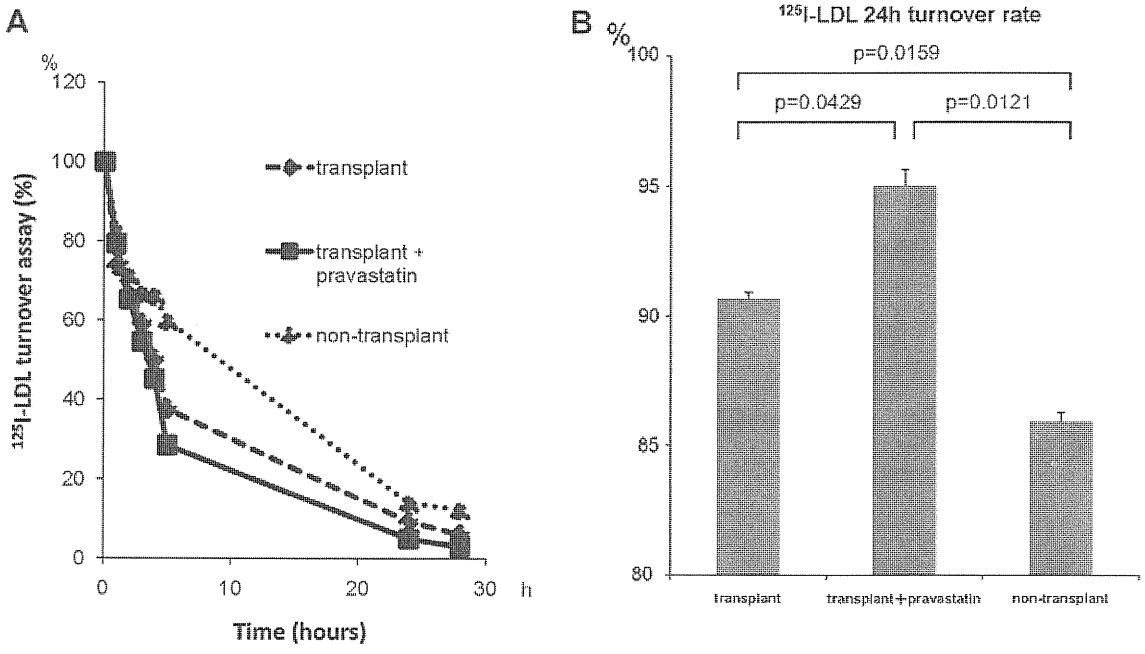

Fig. 3. (A) Rate of clearance of LDL from the serum of WHHL rabbits with and without transplantation of hADMPCs. Animals were injected with ^{125}I-labeled human LDL, and the time course of clearance was monitored following trichloroacetic acid precipitation of serum at time 5 min, 1 h, 2 h, 4 h, 6 h, 24 h and 28 h. Residual ^{125}I-LDL was expressed as percentage of that at 5 min. (B) Differences in the 24-h LDL-clearance rate in pravastatin-treated hADMPC-transplanted group ($n = 4$), hADMPC-transplanted control group ($n = 3$), and non-transplanted control homozygous WHHL group ($n = 3$). Data are mean ± SEM. Differences between mean values before and after treatment in the treated and untreated groups were evaluated using the Student's t-test. A P value less than 0.05 was considered statistically significant.

the LDL receptor synthesis on hepatocytes, thus enhancing the clearance of LDL-cholesterol from the circulation, resulting in lowering serum cholesterol levels [20]. For these reason, pravastatin fail to act in patients with homozygous FH who have no LDL receptor due to the genetic abnormality, and also in the homozygous hyperlipidemic WHHL rabbit, in which pravastatin could show cholesterol-lowering effects in much higher doses of 50 mg/kg/day [23–26]. The substantial fall in serum cholesterol and increased LDL-clearance from the circulation by pravastatin noted in the present study suggest that the hADMPC-derived hepatocyte-like cells both internalize LDL and metabolize cholesterol more efficiently and in concert with pravastatin. The relationship between hypercholesterolemia and coronary heart disease has been well documented, and a reduction in serum total cholesterol of the magnitude demonstrated in the present study is likely to reduce morbidity and mortality rates in patients with homozygous FH [27]. Further studies are needed to tests the potential usefulness of hADMPC-transplantation and simultaneous treatment pravastatin in these patients.

Acknowledgments

This study was supported in part by the Program for Promotion of Fundamental Studies in Health Sciences of the National Institute of Biomedical Innovation (NIBIO), and Kobe Translational Research Cluster, the Knowledge Cluster Initiative, Ministry of Education, Culture, Sports, Science and Technology (MEXT).

References

[1] M.S. Brown, J.L. Goldstein, A receptor-mediated pathway for cholesterol homeostasis, Science 232 (1986) 34–47.
[2] R.J. Havel, N. Yamada, D.M. Shames, Watanabe heritable hyperlipidemic rabbit. Animal model for familial hypercholesterolemia, Arteriosclerosis 9 (1) (1989) 133–138.
[3] T. Yamamoto, R.W. Bishop, M.S. Brown, J.L. Goldstein, D.W. Russell, Deletion in cysteine-rich region of LDL receptor impedes transport to cell surface in WHHL rabbit, Science 32 (1986) 1230–1237.
[4] T. Maruyama, S. Yamashita, Y. Matsuzawa, H. Bujo, K. Takahashi, Y. Saito, S. Ishibashi, K. Ohashi, F. Shionoiri, T. Gotoda, N. Yamada, T. Kita, Research Committee on Primary Hyperlipidemia of the Ministry of Health and Welfare of Japan. Mutations in Japanese subjects with primary hyperlipidemia – results from the Research Committee of the Ministry of Health and Welfare of Japan since 1996, J. Atheroscler. Thromb. 11 (2004) 131–145.
[5] S. Yamashita, H. Bujo, H. Arai, M. Harada-Shiba, S. Matsui, M. Fukushima, Y. Saito, T. Kita, Y. Matsuzawa, Long-term probucol treatment prevents secondary cardiovascular events: a cohort study of patients with heterozygous familial hypercholesterolemia in Japan, J. Atheroscler. Thromb. 15 (2008) 292–303.
[6] J.R. Chowdhury, M. Grossman, S. Gupta, N.R. Chowdhury, J.R. Baker Jr., J.M. Wilson, Long-term improvement of hypercholesterolemia after ex vivo gene therapy in LDLR-deficient rabbits, Science 254 (1991) 1802–1805.
[7] S. Ishibashi, M.S. Brown, J.L. Goldstein, R.D. Gerard, R.E. Hammer, J. Herz, Hypercholesterolemia in low density lipoprotein receptor knockout mice and its reversal by adenovirus-mediated gene delivery, J. Clin. Invest. 92 (1993) 883–893.
[8] K.F. Kozarsky, D.R. McKinley, L.L. Austin, S.E. Raper, L.D. Stratford-Perricaudet, J.M. Wilson, In vivo correction of low density lipoprotein receptor deficiency in the Watanabe heritable hyperlipidemic rabbit with recombinant adenoviruses, J. Biol. Chem. 269 (1994) 13695–13702.
[9] J.M. Wilson, N.R. Chowdhury, M. Grossman, R. Wajsman, A. Epstein, R.C. Mulligan, J.R. Chowdhury, Temporary amelioration of hyperlipidemia in low density lipoprotein receptor-deficient rabbits transplanted with genetically modified hepatocytes, Proc. Natl. Acad. Sci. USA 87 (1990) 8437–8441.
[10] J.R. Gunsalus, D.A. Brady, S.M. Coulter, B.M. Gray, A.S. Edge, Reduction of serum cholesterol in Watanabe rabbits by xenogeneic hepatocellular transplantation, Nat. Med. 3 (1997) 48–53.
[11] M.L. Tejera, J.A. Cienfuegos, P. Maganto, F. Pardo, L. Santamaria, J. Codesal, S. De Andres, J.L. Hernandez, J.L. Castillo-Olivares, Reduction of cholesterol levels following liver cell grafting in hyperlipidemic (WHHL) rabbits, Transplant. Proc. 24 (1992) 160–161.
[12] J. Wang, R. Pollak, A. Bartholomew, Sustained reduction of serum cholesterol levels following allo-transplantation of parenchymal hepatocytes in Watanabe rabbits, Transplant. Proc. 23 (1991) 894–895.
[13] J.C. Wiederkehr, G.T. Kondos, R. Pollak, Hepatocyte transplantation for the low-density lipoprotein receptor-deficient state. A study in the Watanabe rabbit, Transplantation 50 (1990) 466–471.
[14] H. Okura, H. Komoda, A. Saga, A. Kakuta-Yamamoto, Y. Hamada, Y. Fumimoto, C.M. Lee, A. Ichinose, Y. Sawa, A. Matsuyama, Properties of hepatocyte-like cell clusters from human adipose tissue-derived mesenchymal stem cells, Tissue Eng. Part C Methods 16 (2010) 761–770.
[15] H. Okura, A. Saga, Y. Fumimoto, M. Soeda, M. Moriyama, H. Moriyama, K. Nagai, C.M. Lee, S. Yamashita, A. Ichinose, T. Hayamakawa, A. Matsuyama, Transplantation of human adipose tissue-derived multilineage progenitor cells reduces serum cholesterol in hyperlipidemic Watanabe rabbits, Tissue Eng. Part C Methods 17 (2011) 145–154.

[16] M.J. Seo, S.Y. Suh, Y.C. Bae, J.S. Jung, Differentiation of human adipose stromal cells into hepatic lineage in vitro and in vivo, Biochem. Biophys. Res. Commun. 328 (2005) 258–264.

[17] A. Banas, T. Teratani, Y. Yamamoto, M. Tokuhara, F. Takeshita, G. Quinn, H. Okochi, T. Ochiya, Adipose tissue-derived mesenchymal stem cells as a source of human hepatocytes, Hepatology 46 (2007) 219–228.

[18] H. Komoda, H. Okura, C.M. Lee, N. Sougawa, T. Iwayama, T. Hashikawa, A. Saga, A. Yamamoto, A. Ichinose, S. Murakami, Y. Sawa, A. Matsuyama, Reduction of Nglycolylneuraminic acid xenoantigen on human adipose tissue-derived stromal cells/mesenchymal stem cells leads to safer and more useful cell sources for various stem cell therapies, Tissue Eng. Part A 16 (2010) 1143–1155.

[19] H. Okura, A. Matsuyama, C.M. Lee, A. Saga, A. Kakuta-Yamamoto, A. Nagao, N. Sougawa, N. Sekiya, K. Takekita, Y. Shudo, S. Miyagawa, H. Komoda, T. Okano, Y. Sawa, Cardiomyoblast-like cells differentiated from human adipose tissue-derived mesenchymal stem cells improve left ventricular dysfunction and survival in a rat myocardial infarction model, Tissue Eng. Part C Methods 16 (2010) 417–425.

[20] S. Nozaki, T. Nakagawa, A. Nakata, S. Yamashita, K. Kameda-Takemura, T. Nakamura, Y. Keno, K. Tokunaga, Y. Matsuzawa, Effects of pravastatin on plasma and urinary mevalonate concentrations in subjects with familial hypercholesterolaemia: a comparison of morning and evening administration, Eur. J. Clin. Pharmacol. 49 (1996) 361–364.

[21] P. Bjorntorp, M. Karlsson, H. Pertoft, P. Pettersson, L. Sjostrom, U. Smith, Isolation and characterization of cells from rat adipose tissue developing into adipocytes, J. Lipid Res. 19 (1978) 316–324.

[22] J.M. Gimble, A.J. Katz, B.A. Bunnell, Adipose-derived stem cells for regenerative medicine, Circ. Res. 100 (2007) 1249–1260.

[23] F.J. Dowell, C.A. Hamilton, G.B. Lindop, J.L. Reid, Development and progression of atherosclerosis in aorta from heterozygous and homozygous WHHL rabbits. Effects of simvastatin treatment, Arterioscler. Thromb. Vasc. Biol. 15 (1995) 1152–1160.

[24] M. Harsch, A. Gebhardt, A. Reymann, G. Lang, M. Schliack, R. Löser, J.H. Braesen, A. Niendorf, Effects of pravastatin on cholesterol metabolism of cholesterol-fed heterozygous WHHL rabbits, Br. J. Pharmacol. 124 (1998) 277–282.

[25] M. Kuroda, A. Matsumoto, H. Itakura, Y. Watanabe, T. Ito, M. Shiomi, J. Fukushige, F. Nara, M. Fukami, Y. Tsujita, Effects of pravastatin sodium alone and in combination with cholestyramine on hepatic, intestinal and adrenal low density lipoprotein receptors in homozygous Watanabe heritable hyperlipidemic rabbits, Jpn. J. Pharmacol. 59 (1992) 65–70.

[26] M. Shiomi, T. Ito, Y. Watanabe, Y. Tsujita, M. Kuroda, M. Arai, M. Fukami, J. Fukushige, A. Tamura, Suppression of established atherosclerosis and xanthomas in mature WHHL rabbit by keeping their serum cholesterol levels extremely low. Effect of pravastatin sodium in combination with cholestyramine, Atherosclerosis 83 (1990) 69–80.

[27] D. Steinberg, J.L. Witztum, Current concepts. Lipoproteins and atherogenesis, JAMA 264 (1990) 3047–3052.